REPORT DOCUMENTATION PAGE		Form Approved OMB No. 0704-0188

1. AGENCY USE ONLY (Leave blank)	2. REPORT DATE May 15, 1996	3. REPORT TYPE AND DATES COVERED Final Technical Report 1APR93–31MAR96

4. TITLE AND SUBTITLE
Two-dimensional Protein Pattern Recognition in Chemical Toxicity

5. FUNDING NUMBERS
F49620-93-1-0297
61102F
2312 / AS

6. AUTHOR(S)
Frank A. Witzmann, Ph.D.

7. PERFORMING ORGANIZATION NAME(S) AND ADDRESS(ES)

Indiana University
Research & Sponsored Programs
620 Union Drive, Room 618
Indianapolis IN 46202-5167

AFOSR-TR-96
0270

9. SPONSORING/MONITORING AGENCY NAME(S) AND ADDRESS(ES)

AFOSR/NL
110 Duncan Avenue, Suite B115
Bolling AFB DC 20332-0001

10. SPONSORING/MONITORING AGENCY REPORT NUMBER

19960617 121

11. SUPPLEMENTARY NOTES

12a. DISTRIBUTION/AVAILABILITY STATEMENT

Approved for public release;
distribution unlimited.

12b. DISTRIBUTION CODE

13. ABSTRACT (Maximum 200 words)

The mechanisms underlying the effects of chemical toxicity such as cell damage, necrosis, and death, as well as repair, involve changes in the abundance and qualitative character of specific proteins in target tissues and relevant in vitro systems. One way to detect such toxic effects, to determine the mechanism(s) involved in a sepecific effect among a broad range of cellular mechanisms, and to predict the effects of structurally similar compounds, would involve a system that enables simultaneous analysis of greater than 1000 target cell proteins with respect to their response to chemical intoxication. Recognizable patterns of protein alteration so documented would serve as biomarkers of injury or repair, or both. This final technical report documents the progress made during the research period regarding the application of large-scale two-dimensional electrophoresis (2DE) and image analysis to Air Force Toxicologic interests and describes, in particular, the development of prototype tissue 2DE protein databases; multi-species, multi-tissue, and serum 2DE protein map development; and stress protein biomarker development in rodent and human liver samples.

14. SUBJECT TERMS
electrophoresis, two-dimensional; protein mapping; protein databases; liver; kidney; serum; rat; human; mouse; toxicity

15. NUMBER OF PAGES

16. PRICE CODE

17. SECURITY CLASSIFICATION OF REPORT	18. SECURITY CLASSIFICATION OF THIS PAGE	19. SECURITY CLASSIFICATION OF ABSTRACT	20. LIMITATION OF ABSTRACT

DTIC QUALITY INSPECTED 1

DISCLAIMER NOTICE

UNCLASSIFIED

Technical Report
distributed by

**DEFENSE
TECHNICAL
INFORMATION
CENTER**

DTIC Acquiring Information-
Imparting Knowledge

Cameron Station
Alexandria, Virginia 22304-6145

UNCLASSIFIED

**THIS DOCUMENT IS BEST
QUALITY AVAILABLE. THE
COPY FURNISHED TO DTIC
CONTAINED A SIGNIFICANT
NUMBER OF PAGES WHICH DO
NOT REPRODUCE LEGIBLY.**

TWO-DIMENSIONAL PROTEIN PATTERN RECOGNITION IN CHEMICAL TOXICITY

Frank A. Witzmann, Ph.D.

Molecular Anatomy Laboratory
Department of Biology
Indiana University Purdue University Columbus
4601 Central Avenue
Columbus IN 47203

May 1996

FINAL TECHNICAL REPORT FOR PERIOD 1 APR 93 THROUGH 31 MAR 96

TABLE OF CONTENTS

Abstract

The mechanisms underlying the effects of chemical toxicity such as cell damage, necrosis, and death, as well as repair, involve changes in the abundance and qualitative character of specific proteins in target tissues and relevant *in vitro* systems. One way to detect such toxic effects, to determine the mechanism(s) involved in a specific effect among a broad range of cellular mechanisms, and to predict the effects of structurally similar compounds, would involve a system that enables simultaneous analysis of > 1,000 target-cell proteins with respect to their response to chemical intoxication. Recognizable patterns of protein alteration so documented would serve as biomarkers of injury or repair, or both. This final technical report documents the progress made during the research period regarding the application of large-scale two-dimensional electrophoresis (2DE) and image analysis to Air Force toxicologic interests and describes, in particular, the development of prototype tissue 2D protein databases; multi-species, multi-tissue and serum 2D protein map development; and stress protein biomarker development in rodent and human liver samples.

The animals used in this study were handled in accordance with the principles stated in the Guide for the Care and Use of Laboratory Animals, prepared by the Committee on Care and Use of Laboratory Animal Resources, National Research Council, DHHS, National Institute of Health Publication #86-23, 1985, and the Animal Welfare Act of 1966, as amended.

INTRODUCTION

The efforts of this laboratory during the research period involved the development of an approach directed at promoting a predictive toxicology based on target tissue protein pattern recognition. By using large-scale two-dimensional electrophoresis of proteins (2D-PAGE) combined with computerized image analysis, methods for comparing computer processed 2D-protein pattern alterations in various target tissues induced by specific chemical agents formed the basis for this investigation. Observed alterations were used to indicate and comparatively assess toxicity by detecting specific patterns of protein alteration. Concurrently, previously established two-dimensional protein pattern databases for various rodent target tissues were developed and expanded.

The effectiveness of the large-scale 2D-PAGE technique used in this laboratory resulted from the resolution of >1,000 cellular proteins in a single tissue sample, first based on the proteins' content of acidic and basic amino acids (isoelectric focusing) and second by molecular weight (SDS electrophoresis). In combination, these two separation techniques produced two dimensional protein patterns unique for each tissue or group of cells tested. Individual proteins within the pattern were analyzed for alterations in volume (density), charge, and molecular weight. Changes in volume or spot density reflected alterations in a protein's abundance and suggested up- or down-regulation of the genome or altered protein turnover rates. Charge modifications suggested either posttranslational modification such as phosphorylation, ribosylation, conjugation or amino acid substitutions resulting from point mutations in the genome.

Regardless of chemically-induced changes, the well-resolved 2D protein patterns, or 2D protein maps (fingerprints), generated in this investigation provided a variety of patterns containing 1000-2000 proteins and thus a significant source of information regarding the health/activity of a particular cell/tissue type and its response to toxic insult. This Final Report summarizes the progress made during the research period in the following areas: 1) Perfluorocarboxylic acid toxicology (comparative peroxisome proliferator toxicity, pattern alterations in 2D protein maps); 2) 2D Protein Database Development; 3) Resolution of sample proteins with pI > 7.0 via first-dimension immobilized pH gradient electrophoresis (IPG-DALT); and 4) Other toxicant effects on protein patterns from hepatic and extrahepatic targets in different rat strains and mice

Following a detailed description of methodology and instrumentation used in these studies, individual results will be presented, in brief, and pertinent data (*i.e.* spot maps, tables, and graphs) will be presented in several appendices.

MATERIALS AND METHODS

Animal Treatment. Male Sprague-Dawley rats (200-225 g) were obtained from Harlan Sprague-Dawley Inc. and male Fisher-344 rats (225-250g) were obtained from Charles River Breeding Labs. All rats were housed individually, maintained over sawdust bedding free of any chemical contaminants for 10 days on a 12 hr photoperiod. A temperature of 21°C and 50% relative humidity were maintained at all times. The animals had free access to water and commercial rat chow (diet no. 7001, Teklad, Madison WI) before, during, and after treatments.

The following peroxisome proliferators were studied in F344 rats. Perfluoro-n-decanoic acid (PFDA) and perfluoro-n-octanoic acid (PFOA), Aldrich Chemical Company (Milwaukee WI), were dissolved in propylene glycol and water, 1:1 by volume, and concentration adjusted so that the dose

volume did not exceed 0.5 ml. Rats were injected intraperitoneally with the above solutions so that exposures were as follows: 2 mg (n=5), 20 mg (n=5), and 50 mg PFDA/kg body weight (n=9), single injection, animals sacrificed on day 8 of exposure; 50 mg PFDA/kg body weight (n=5), single injection, 30 days after exposure; and 150 mg PFOA/kg body weight (n=8), single injection, animals sacrificed on day 3 of exposure. Clofibrate (ethyl- -*p*-chlorophenoxy-isobutyrate), Sigma Chemical Co. (St. Louis MO), was administered as neat oil, 250 mg clofibrate/kg body weight, single intraperitoneal injection on each of 3 successive days, animals sacrificed on day five of exposure (n=10). Di(2-ethylhexyl)phthalate (DEHP), Aldrich Chemical Company (Milwaukee WI), was administered as neat oil via oral gavage, 1200 mg/kg per day, animals sacrificed on day 5 of exposure (n=3). Matched control rats were vehicle injected and pair-fed (PFC; n=7) to control for aphagia, a prominent characteristic of high-dose perfluorocarboxylic acid exposure. One group (Ad Lib; n=5) served as free-eating controls. It is important to emphasize that the route and level of toxicant exposures described above have previously been shown to result in maximal peroxisome proliferation with minimal lethality in male rats (14-15).

In the thioacetamide (TA) study, Sprague-Dawley rats were divided into 4 major groups and treated intraperitoneally with TA (50, 150, 300, 600 mg/kg) dissolved in water. The respective controls received water (1 ml/kg) used as the vehicle for TA administration. Portions of the liver from each diethyl ether anesthetized rat were collected at various intervals (2, 4, 6, 8, and 16 hr) after TA or vehicle administration.

Trichloroethylene (TCE) was administered by corn oil gavage to male B6C3F1 mice 5 days per week for 8 weeks at doses of 0 (vehicle), 400, 800, 1200 mg/kg. Liver samples (100-250 mg) were frozen at -70° C for solubilization later.

In conjunction with the Army Medical Research and Development Command component of the Tri-Service Toxicology Consortium at Wright-Patterson AFB, male Sprague-Dawley rats (225-250 g) received 20, 100, or 200 mg AND/100 ml in drinking water continuously for 90 days. Following exposure, the rats were sacrificed and mixed arteriovenous blood samples obtained.

Sample Preparation. For the rat liver, a 0.5 g piece was removed, and then minced and homogenized in 8 volumes (4 ml) of a lysis buffer containing 9 M urea (BDH Chemical Ltd., Poole, UK), 4% CHAPS (3-[(3-cholamidopropyl)-dimethylamonio]-1-propanesulfonate) (CALBIOCHEM, La Jolla CA), 2% DTE (dithioerythritol) (BIO-RAD, Richmond CA) and 2% ampholytes (pH 8-10.5) , pH 9.5 (Sigma Chemical Co., St. Louis MO) for two-dimensional (ISO-DALT®) electrophoresis. One whole kidney (approx. 1 g/rat) was surgically removed, blotted, trimmed of excess fat and epithelial membranes and prepared in a manner identical to the liver samples.

Mouse liver samples were treated similarly, adding 4 volumes of lysis buffer to the frozen sample and mincing, followed by ground-glass homogenization. After solubilization at room temperature for 120 min, samples were centrifuged at 100,000 x *g* for 30 min to remove insoluble materials and nucleic acid and the supernates stored at -70° C.

Rat brain (cerebrum) was obtained from untreated rats, rinsed with ice-cold saline, weighed, and homogenized in 4 volumes of the same buffer used for liver. Brain homogenates were solubilized for 120 minutes at room temperature, centrifuged at 100,000 x *g* for 30 min and the supernates stored at -70° C.

Sprague-Dawley serum samples (from clotted blood samples) were solubilized by adding 4 volumes of a lysis buffer containing 0.04 M CHES, 2% SDS, 1% DTT (dithiothreitol) and 10% glycerol for 2D electrophoresis [1]. Samples were solubilized at room temperature with periodic vortexing and finally stored at -70° C until use.

Two-Dimensional Electrophoresis. Sample proteins were resolved by 2D electrophoresis using the 20 x 25 cm ISO-DALT® 2D gel system operating with 20 gels per batch. All first dimension isoelectric focusing (IEF) gels were prepared using the same single standardized batch of ampholytes (BDH 4-8) selected for rat database work. Ten microliters of solubilized protein sample were applied to each gel, and the gels were run for approximately 25,000 volt-hours (depending on the sample) using a progressively increasing voltage protocol implemented by a programmable high voltage power supply.

An Angelique® computer-controlled gradient casting system was used to prepare second dimension SDS gradient slab gels in which the top 5% of the gel was 11%T acrylamide, and the lower 95% of the gel varied linearly from 11% to 18%T. Each gel was identified by a computer-printed filter paper label polymerized into the gel. First dimension IEF tube gels were loaded directly onto the slab gels without equilibration, and held in place by polyester fabric wedges to avoid the use of hot agarose. Second dimension slab gels were run in groups of 20 in a DALT slab electrophoresis tank thermostated at 10°C. The run lasted approximately 18 hr at 160V.

Following SDS electrophoresis, slab gels were stained for protein using a colloidal Coomassie Blue G-250 procedure in covered plastic boxes, with 10 gels per box. This procedure involved fixation in 1.5 liter of 50% ethanol/2% phosphoric acid overnight, three 30 minute washes in 2 liter of cold tap water, and transfer to 1.5 liter of 34% methanol/17% ammonium sulfate/2% phosphoric acid for one hour followed by addition of a gram of powdered Coomassie Blue G-250 stain. Staining required approximately 4 days to reach equilibrium intensity. This method typically resolved 1,200-1,500 proteins in a 10μl sample.

Quantitative Computer Analysis. Each stained slab gel was digitized at 125 micron resolution, using an Eikonix 1412 scanner and high-intensity light box. Raw, digitized gel images were archived on high-density DAT tape (or equivalent storage media) and a greyscale videoprint prepared from the raw digital image as hard-copy backup of the gel image. Each 2DE gel was processed using the Kepler software system with procedure PROC008 which provided a spotlist giving position, shape and density information for each detected spot. This procedure made use of digital filtering, mathematical morphology techniques and digital masking to remove background, and used full two-dimensional least-squares optimization to refine the parameters of a 2D Gaussian shape for each spot. Processing parameters and file locations were stored in a relational database, while various log files detailing operation of the automatic analysis software were archived with the reduced data.

The specific experiment package was constructed using the Kepler® experiment definition database to assemble groups of 2DE patterns corresponding to the various control and experimental groups associated with each experiment. Each pattern was matched to the appropriate "master" pattern, thereby providing future linkage to a tissue protein 2DE database under development. The Kepler® software system used provides the capacity to construct experiments containing hundreds of gels that can also be analyzed as a unit, with up to 99 gels displayed on screen at one time for comparative purposes. Consequently, the routine analysis of hundreds of sample gels was quite practical.

The groups of gels making up an experiment were then scaled together (to eliminate quantitative differences due to gel loading or staining differences) by a linear procedure based on a selected set of spots. These spots were selected by the GOODSCALE procedure [2], which selects spots which are Gaussian converged, have a good initial intra-group coefficient of variation (CV), have a good (non-elongated) shape, an integrated density between certain limits (avoiding very small or overloaded spots), and were detected on almost all gels of the set.

Statistical analyses. Groupwise statistical comparisons (Student's t-test) were made graphically and interactively and the results displayed in montage format using the KPL42 module. Graphical results of individual spot statistics and spot maps were printed in postscript on a microLaser Plus printer (Texas Instr.) while raw gel images and spot profiles were printed using a 64 level greyscale videoprinter (Codonics). Spot volume information generated by Kepler™ was exported to a PC for one-way ANOVA and the SNK multiple comparison test using SigmaStat (Jandel).

In specific studies, the level of charge modification was determined by calculating the Charge Modification Index (CMI) [3] for each sample. This index describes the overall average number of charges added per protein molecule examined.

RESULTS & DISCUSSION

Perfluorocarboxylic acid toxicology (comparative peroxisome proliferator toxicity). As a result of protein identifications made during the research period, it was possible to characterize PFOA and PFDA hepatotoxicity in comparison to the chemically distinct peroxisome proliferators clofibrate and DEHP. This section summarizes the effect of *in vivo* exposure to these compounds in rats. Alterations in the expression of hepatic sulfotransferases and stress proteins, with particular attention to protein charge modification, are discussed.

In Appendix A, Figure 1 illustrates the two-dimensional protein map of F344 male rat liver whole homogenate. This 2D map is a master pattern, a composite of all proteins detectable in the liver that constitute this experiment. The master pattern serves as a reference for comparison of current and future experimental rat liver patterns where virtually identical running conditions were or will be used. Each protein spot is arbitrarily assigned a master spot number (MSN) connoting that protein's identity in the database for F344LIVER.

Sulfotransferases can be categorized into two major subfamilies (ST1 and ST2) according to their substrate specificities and cDNA-derived amino acid sequence homologies: 1) ST1 includes phenol sulfotransferases (PSTs) that comprise a number of STs active against a range of phenolic xenobiotic and endogenous compounds including estrogen sulfotransferase (ST1E) and 2) ST2 includes hydroxysteroid sulfotransferases (HSTs or alcohol STs) which sulfate steroid hormones, bile acids and xenobiotic alcohols [4]. The rat ST1 currently identified via cDNA clones are ST1A1 (PST-I) and ST1C1 (HAST-I). The ontogeny and gender-dependent distribution of rat PST indicates that PST activity develops after birth, attaining a maximum at 30-40 days of age and that PST activity in the adult male is approximately threefold higher than in the adult female rat [5]. Various forms of sulfotransferase have also been demonstrated in the human where the degree of ST1 expression is genetically variable in blood platelets and is dependent on the level of enzyme protein [6]. As these ST enzymes play important roles in the metabolism of xenobiotics and are active in the inter-regulation of steroid production, their alteration *in vivo* is also of importance. The labeled spots identif
y the *x, y* coordinate position of ST1A1, ST2A1, and ST1C1 and their charge variants. Molecular weight and pI's, both calculated [7] and estimated based on 2D gel calibration, of the identified sulfotransferases are listed in Table 1 on the next page.

Verification of the protein spot identified as MSN176 from the F344LIVER pattern as ST1A1 was based first on its precise positional homology relative to a spot found in the F344MST3 (v1.5, 1995) rat liver master pattern generated by Large Scale Biology Corp. and second on its immunodetection using anti-rat paracetamol ST antibody. This protein spot was extracted from replicate gels, the peptide

sequence determined after tryptic digestion [CPGVPSGLETLEETPAPR], and the resulting sequence (aa 82-99) matched to a protein identified as rat liver aryl sulfotransferase PST-1 (PIR accession number S10329) [8]. The calculated pI (6.40) and MW (33,736) of this protein is in concordance with our own estimates from our standardized 2D map and its abundance in control samples represents approximately 0.6% of the total protein resolved on our gels. This renders ST1A1 a relatively abundant protein in the rat liver whole homogenate and a notable spot on the pattern. Comparatively, β and δ actin, with recognizable 2D coordinates and nearly invariable appearance on 2D gels in the liver, together represent approximately 0.9% of the total resolved protein. The anti-rat paracetamol ST antibody recognized MSN176 and 396 only, confirming the sequence identification and identifying MSN396 as a charge variant of MSN176.

Table 1. Rat liver sulfotransferases studied.

Sulfotransferase	ID	MSN	pI*	MW*	PIR #	pI seq	MW seq	x-react anti-paracet. antibody	%ST1A1 sequence homology	x-react anti-ST2A1 antibody	%ST2A1 sequence homology	x-react anti-ST2E1 antibody	%ST1E2 sequence homology
paracetamol ST (PST-I)	ST1A1	176	6.84	35,195	S10329	6.41	33,736	yes	100	yes	34	yes	49
		396	6.62	35,105	--	--	--	yes		no		no	
N-hydroxyarylamine ST (HAST-I)	ST1C1	166	6.31	34,353	A49098	6.11	35,723	no	50	yes	36	yes	46
		406	6.04	34,226	--	--	--	no		no		yes	
hydroxysteroid ST (HST)	ST2A1	180	7.29	36,272	A34822	8.03	33,251	no	34	yes	100	no	34
		193	7.04	36,371	--	--	--	no		yes		no	
		287	6.76	36,308	--	--	--	no		yes		no	

*F344LIVER estimates calculated as described in text; PIR estimates based on rat ST protein sequences; x-react connotes cross-reactivity with the ST;

The identification of MSN166 and 406 as ST1C1 was based on 1) precise positional homology relative to a spot (identified as HAST-I by sequence analysis) found in the F344MST3 (v1.5, 1995) rat liver master pattern generated by Large Scale Biology Corp. and 2) its reaction with anti-ST1E2 and anti-ST2A1 antibodies. The immunoreactivity of ST1C1 to the anti-ST1E2 and anti-ST2A1 antibodies is likely a result of its significant sequence homology (see Table 1) with these two sulfotransferases. Interestingly, ST1E2 antibody recognized both charge forms of ST1C1 while anti-ST2A1 antibody recognized only the parent (right-most, most basic form) of ST1C1.

Protein spots MSN180, 193, and 287 were identified as three charge-variants of ST2A1 by their strong immunoreactivity with the anti-ST2A1 antibody. This antibody also reacted with the uncharged, parent forms of ST1A1 and ST1C1. As Figure 2 illustrates, hepatic ST1A1, ST1C1 and ST2A1 display charge microheterogeneities, e.g. the appearance of at least one charge variant in addition the parent charge form (most basic form). Detection of such isoelectric point variation by 2DE is common and reflects posttranslational modification, (e.g. phosphorylation, glycosylation, deamination, or sulfation) associated with normal cellular processing and regulation of certain proteins. Modifications that occur as a result of adduct formation are characterized by the appearance of large numbers of charge variants (charge-trains) as previously demonstrated [3].

Calculation of the protein Charge Modification Index (CMI) (7) of these ST's revealed no change in microheterogeneity by any of the treatments. This is particularly notable given the susceptibility of rat hepatic ST2A1 to charge variations as a function of gender and age [9-10].

Sulfotransferase abundance (pooled abundances of charge variants detected for each sulfotransferase) as a function of treatment group is shown in Figure 3. ST2A1 abundance was

statistically unaffected by any of the peroxisome proliferators used. ST1A1 and ST1C1 abundance was significantly decreased by PFDA treatment, an effect that persisted for 30 days after the single-dose exposure. Lower doses of PFDA significantly altered neither ST1A1 nor ST1C1 abundance, although the 20 mg/kg protein abundances suggested a downward trend in ST1A1 and ST1C1 abundance. PFDA's 8-carbon analog, PFOA, also exhibited a trend toward ST1A1 down regulation. In fact, PFOA exposure significantly reduced ST1C1 abundance.

Interestingly, food-restriction that accompanied pair-feeding (PFC) resulted in a significant induction of ST1A1, but no other ST. ST expression and activity have been shown to decline following dietary administration of 2-acetylaminofluorene [11], a compound O-sulfonylated by HAST [12], as a result of various putative mechanisms. It is possible that similar effects may be responsible for the down-regulation of ST1A1 and ST1C1 in the present study. Unfortunately, the perfluorocarboxylic bioactivation in the liver has not been demonstrated. However, the absence of DEHP and clofibrate effects combined with PFDA's persistent effect (up to 30 da.) and its accumulation in the liver, even after a single exposure [13], suggests a mechanism unrelated to general PP toxicity. The observed down-regulation of these ST's is significant with respect to their normal detoxification activities and its potential correlation to carcinogenesis [11] warrants further study. The present investigation supports previous studies that demonstrate the unique features of perfluorocarboxylic acid toxicity, relative to "classic" peroxisome proliferators. The data also support the use of 2D protein-mapping of ST's as markers of chemical toxicity.

This technology was also applied to the development of a more expanded system of two-dimensional electrophoretic protein markers that can be used in toxicologic screening and mechanistic studies. To this end, a set of specific proteins that are constitutively expressed in recognizable 2DE patterns in toxicologic target tissues were previously identified and mapped [14]. These stress proteins, such as the heat shock and glucose-regulated proteins (hsp and grp), are highly conserved, respond to both thermal and metabolic stress and are known to be intimately involved as chaperones in the biogenesis and disposition of cellular protein products. Furthermore, this group of related proteins have increasing potential relevance in environmental toxicology, clinical medicine, and human health.
The characteristics of heat shock proteins and other molecular chaperones and their connection to stress tolerance have been reviewed [15-17].

2DE maps displaying the previously determined [14] x, y coordinate positions of the stress proteins examined in liver and kidney are shown in Figures 1 and 4, Appendix A, respectively. Table 2, Appendix A presents total abundance (sum of all charge variants) of stress proteins analyzed as a percent of *ad lib* fed group's abundance. In the liver, three stress proteins, hsp60, hsp70, and grp75 were induced as a result of pair feeding (complete food restriction) when compared to the *ad lib* fed group. Pair-feeding (essentially food restriction) was necessary to control for complete aphagia and subsequent body weight loss previously shown to accompany PFOA (unpublished) and 50 mg/kg PFDA [13] exposures and prominently elicits a metabolic stress on the liver. In contrast, the 2 mg/kg and 20 mg/kg PFDA exposures were not accompanied by aphagia. Consistent with previous observations [13], rats in the PFDA 50 mg/kg, 30 day group began to eat on day 12 following the single exposure and were eating normally for the last two weeks of the 30 day period. Therefore, valid comparisons of PFOA-treated and PFDA-treated (50 mg/kg, 8 da) group means to untreated animals must be made with the pair-fed group while all other free-eating treated groups can be compared to the *ad lib* group.

In contrast to the liver, food restriction failed to induce any of the stress proteins observed in the kidney. In fact, the only renal alteration associated with this condition was a decrease in hsp32

abundance. PFOA exposure caused inductions in liver hsp60, hsc70, hsp70, and grp75, but only to the extent that they exceeded the *ad lib* but not the pair-fed group. In contrast, renal hsp70, grp75, and grp78 were all significantly induced above pair-fed control values. Low-dose PFDA exposure, 2 mg/kg, had no effect on either target tissue. The ten-fold higher PFDA exposure (20 mg/kg) induced hepatic hsp60 relative to pair-fed controls while hsc70, hsp90, and grp75 abundances were all significantly higher than those in the *ad lib* group. Again, PFDA at this exposure level had little effect on the kidney. Only hsp32 was altered significantly and then only relative to the pair-fed control, where its abundance had diminished during pair-feeding.

High dose PFDA exposure (50 mg/kg) for 8 days resulted in significantly more stress protein alterations than the other lower-dose treatments. Hepatic hsp60, and grp75 abundances were increased by this intoxication (relative to the pair-fed group) while PDI was lower than the pair-fed level and ER60 abundance was reduced by nearly one-half. Thirty days after the single 50 mg/kg PFDA exposure, grp75 was still significantly elevated, hsp60 and grp78 remained above *ad lib* levels, and ER60 and hsp32 were significantly reduced. PDI abundance was also significantly reduced below both pair-fed and *ad lib* levels, a trend started after 8 days of exposure.

In view of the numbers of stress proteins altered and the extent of their alteration (Table 2) where renal stress proteins were less effected by PFDA at the single 50 mg/kg dose and only hsp60, hsp70, and grp75 were induced. PFDA's effect on the kidney is somewhat less conspicuous than PFOA's. The PFDA effect was also far less persistent in the kidney, where after 30 days, only hsp32 was altered and then only relative to the pair-fed group where this protein's abundance had been reduced by pair-feeding. This phenomenon, along with the persistence in PFDA's hepatic effects, probably relates to its long-term bioavailability in the liver [13] in contrast to the kidney where it's excretion may likely reduce its long-term effects. It is important to note here that the rats in the 30 day exposure were free-eating for 2 weeks prior to sacrifice and therefore display few of the effects of food restriction. The hsp32 data support this notion.

The results demonstrate a preferential hepatic effect of PFDA exposure and renal effect of PFOA, with respect to stress protein alterations. However, in both targets, the mitochondrial stress proteins hsp60 and grp75 were most susceptible to the PFOA/PFDA exposures suggesting a preferential effect of these compounds on the mitochondrion. Nevertheless, stress proteins in all cellular compartments were affected by PFOA and PFDA exposure. Because significant alterations in these proteins was induced by food restriction, 2DE data from experiments where pair-feeding is necessary must be interpreted with caution. The results suggest that with further study of a broad range of chemical toxicants, this group of protein biomarkers may be of general use in toxicologic investigation.

A second perfluorocarboxylic acid effect, observed in a particular stress protein, concerned a statistically significant chemical-charge modification of a prominent hepatic endoplasmic reticulum protein, immunoglobulin heavy chain binding protein (Grp78/BiP). The alteration of this soluble, luminal protein is of particular interest because Grp78 acts as a molecular chaperone with a significant role in the disposition of nascent proteins. Specifically, in its dephospho form, Grp78/BiP prevents the secretion of mutant or defective proteins from the ER. The unique nature of Grp78's modification and its susceptibility only to the perfluorocarboxylic acids studied reflects the complex and varied nature of PP toxicity.

This specific experiment focused on Grp78/BiP and Hsp60, whose identities and appearance as trains of charge variants were confirmed immunologically (and by comigration of purified Grp78/BiP). In the 2D electrophoretic system, proteins that ordinarily exist as "microheterogeneities" can be correctly

assumed to have undergone some form of post-translational modification such as phosphorylation, glycosylation, deamidation/amidation or conjugation. These microheterogeneities are observed as trains of spots with similar molecular weight trailing to the left (acidic) end of the slab. Typically, the most basic component of this "charge train" is the "parent" or unmodified form.

Although the master pattern in Figures 1 and 2 show 5 distinct Grp78/BiP charge variants, only those 3 with the most basic pI are normally expressed in the untreated liver. The additional 2 acidic charge variants of Grp78 have been observed almost exclusively in PFDA-treated rats. Hsp60 normally appears as the three spots shown on the master pattern; no additional charge variants (neither acidic nor basic) have been observed in our experiments.

Modifications induced by PFDA exposure involve the addition of new, negatively charged proteins to the normal pattern. In the pair-fed control protein pattern, Grp78/BiP exists as three and a minor fourth charge variants in pair-fed control rat livers. In contrast, a typical pattern representing the PFDA (50 mg/kg, 8 da) treatment group has 5 charge variants. This indicates a distinct leftward shift in protein abundance, from the most basic parent species to more acidic forms. In contrast to Grp78/BiP, Hsp60 undergoes a proportional induction of all charge variants as a result of PFDA exposure and not a specific acidic charge-shift. Total protein abundance of Grp78/BiP across the experimental groups (calculated by summing the individual abundances of all charge forms) was slightly increased by the PFDA (50 mg/kg, 8 da) exposure only ($F = 4.11$, $p < .001$), while all experimental manipulations, with the exception of PFDA (2 mg/kg), caused a significant induction of total Hsp60 abundance ($F = 15.52$, $P < .001$). Hsp60 was thus chosen to reflect a protein *quantitatively* altered by chemical exposure in distinct contrast to the *qualitative* alterations detected in Grp78/BiP.

A comparison of the CMI from all treatment groups is shown in the table below:

Table 3. Charge Modification Index (CMI) of Grp78/BiP and Hsp60

Treatment	n	Grp78/BiP CMI	Grp78/BiP Treatment - PFC	Hsp60 CMI	Hsp60 Treatment - PFC
Pair-fed Control (PFC)	6	-0.65	NA	-0.49	NA
Ad lib fed Control	9	-0.62	0.03	-0.34	0.15
PFOA (150mg/kg)	8	-0.82	0.17	-0.32	0.17
PFDA (2mg/kg)	5	-0.75	0.1	-0.41	0.08
PFDA (20mg/kg)	5	-0.96	0.31	-0.46	0.03
PFDA (50mg/kg; 8da)	9	-1.3*	0.65*	-0.4	0.09
PFDA (50mg/kg;30da)	5	-1.36*	0.71*	-0.45	0.04
Clofibrate	10	-0.86	0.21	-0.45	0.04
DEHP	3	-0.61	0.04	-0.43	0.06

Values shown above are group means; comparisons were made via one-way ANOVA (Grp78/BiP, *F=12.638, p<0.001; Hsp60, F=3.433, n.s.). Pairwise multiple comparisons of Grp78 by Student-Newman-Keuls method (p<0.05) revealed that PFDA exposures, 50mg/kg, (8da and 30da)differed significantly from all other groups but not from each other. No other significant differences were observed.

Based on this calculation, 8 day exposure to PFDA (50mg/kg) was associated with a significant modification of Grp78/BiP by the addition of negative charges. Furthermore, this modification persisted

virtually undiminished at 30 days following the single exposure. PFDA also had a lesser, statistically insignificant effect at 20 mg/kg as did PFOA. Comparatively, clofibrate did not significantly alter CMI although the minor elevation (0.21) resembled that associated with PFOA (0.17), while DEHP exerted no effect whatsoever. In fact, none of the treatments elicited a change in CMI greater than 0.17.

The statistically significant alteration in the small population of charge variants of Grp78/BiP associated only with high-dose PFDA exposure and the induction of aggregate Grp78/BiP supports the view that, while PFDA is a potent peroxisome proliferator, its mechanism may be very different from that of classic PPs like clofibrate and DEHP. To interpret the meaning of the observed protein modifications and how PFDA's toxic mechanism may be different, one must consider BiP's normal cellular function. As mentioned earlier, BiP is believed to be involved in the processing of secretory proteins and the recognition, retention and degradation of misfolded or misassembled proteins in the ER.

In carrying out this function, BiP is phosphorylated [18] and ADP ribosylated [19]. It is also known that both phosphorylation and ribosylation are associated with nonfunctional or inactive BiP [18, 20]. Thus the cell may regulate its protein secretory activity not necessarily by synthesizing more or less BiP but rather by post-translational modification of existing protein. Since the dephosphoprotein and deribosylated forms are the active forms, our observations of leftward, acidic shifts from the native, most basic charge form of BiP suggest that PFDA may cause the inactivation of BiP despite increasing its abundance. This assumes that the observations are indeed ribosylation, phosphorylation, or both.

It is unlikely that the present alterations are the result of adduct formation such as the methapyrilene effects observed previously in F344 rat liver [3] and *in vitro* [21]. In those studies, methapyrilene-protein conjugation resulted in the appearance of as many as 6 additional charge variants of Hsp60 and a change in CMI of over 1.00 (-0.42 to -1.52). Regarding Grp78/BiP in the present study, a large number of new charge variants do not appear as a result of PFDA intoxication. Instead, an increase in the abundance of those occurring naturally and a significant decline in the abundance of the "parent" form occurs. This results in a comparatively modest elevation of CMI, from 0.65-0.71 (-0.65 to -1.30 or -1.36), an acidic shift more representative of enhanced ribosylation or phosphorylation effects. That this effect should persist even 30 days after single-dose exposure relates to the inability of the liver to metabolize PFDA [22, 23] and the fact that PFDA accumulates there more than in any other tissue [13].

Whether this peculiar PFDA effect on Grp78/BiP is *1)* a part of a generalized stress response (i.e. oxidative stress), as suggested by the induction of total Hsp60, that results in elevated phosphorylation or (ribosylation) of BiP to stop the export of certain proteins from the hepatic ER or *2)* a specific, primary effect attributable to PFDA intoxication is being studied and will be the subject of a pending report. Nevertheless, PFDA exposure results in distinctive changes in this important cellular protein in direct contrast to the other peroxisome proliferators studied. These data also demonstrate that one need not necessarily look for a increase or decrease in the abundance of stress proteins such as those seen here and in other studies, but rather one can observe subtle qualitative changes that cannot be detected easily via other means.

Although PFDA's specific mechanism and peroxisome proliferative mechanisms in general have not been elucidated from these data, this study has confirmed our expectation that high-resolution 2D electrophoresis in combination with image analysis can reveal subtle biochemical changes associated with important xenobiotic effects. As more proteins are identified in our database of rat liver 2D patterns and those of others, it will be possible to assess enzyme induction, modification, and protein conjugation and to explore cellular metabolic pathways associated with specific intoxications (*i.e.* peroxisomal - oxidation).

The data presented conform to the criteria established for systematic use of 2D electrophoresis in toxicology [24] in that we have detected a reproducible effect that is characterized by detectable changes at the molecular level, changes that are specifically associated with a molecular effect that enables one to differentiate various classes of mechanisms. Further investigation, already underway, will ensure that there is a firm basis for expecting that the molecular changes can be interpreted in a way that helps explain not only the details, but also the significance of the events observed.

Database Development. Appendix B contains a representative sample of the F344 Rat Liver Protein Database under continuous development in the principal investigator's laboratory. This database contains all protein spots comprising the F344LIVER_1 map presented in Appendix A. As the spreadsheet shows, the proteins are listed by MSN, although they can be sorted by any variable represented in the table. This table lists all 107 protein spots currently identified. The 107 known identities remain a small fraction of the 1469 protein spots detected in the rat liver and present in the 2D master pattern. Relative to other databases in other laboratories published in *Electrophoresis* Journal, this number is quite comparable. In last year's technical report, 84 proteins had been identified while in 1993, 59 identifications were reported. The continued expansion of this database, as well as similar databases for kidney, serum, brain and ultimately cultured cells and tissue slices, is an ongoing project. Improvements in global internet capabilities will speed up the identification process by making similar database comparisons less complicated thus enabling more rapid and more precise determinations of toxic mechanism.

To calibrate x and y coordinates of our 2DE master patterns, we calculated the pI and MW of proteins with known 2DE coordinate positions, as described [7, 25]. These included calmodulin (pI 3.85) to catalase (pI 7.07) as well as 20 others with pIs distributed within that range. Using these pIs, with their corresponding x coordinates, a standard fitted curve was calculated using multivariate curve-fitting software (Tablecurve, Jandel). The pI estimate for each protein in the database was then calculated based on the resulting equation. A similar method was applied to molecular weight estimation. The same proteins used in pI estimation were used to calculate MW. The identified protein MW was obtained directly from the SWISS-2DPAGE database where it is calculated from amino acid composition based on the SWISS-PROT entry. As before, a standard fitting curve was calculated from MW and y coordinate data. Because we use an 11-17% acrylamide gel gradient for 2nd dimension separation, the fitting curve was not limited by a predetermined model. Rather, we selected the equation that described a curve that best fit the data from the many generated by Tablecurve. The y coordinate data from each protein in the database was then used to estimate MW.

Using the same approach for proteins contained in the PIR, SWISS-PROT and other databases, we determined the calculated pI and MW for over 800 sequenced proteins whose identity and tissue expression may be relevant to ongoing experiments. Using acid-base equations for pI calculations in a spreadsheet format (Large Scale Biology Corp. - proprietary software), protein pI can be calculated easily if the exact amino acid composition is known. The objective is to calculate for each protein of interest, the pH at which point the protein has a net electrical charge of zero. The only components of a protein that contribute to the charge are those side-groups of amino acids possessing acid-base properties. Using an iterative process and taking into consideration the blocked or modified N-termini, accurate determination of pI is underway. Protein MW is also easily calculated based on amino acid composition. Protein MW is determined by simply adding the molecular weights of the amino acids

comprising that protein and subtracting 18 X (n-1) to account for the loss of a water molecule per peptide bond formed.

A sample of the 800+ proteins in the pI and MW Database is presented on the spreadsheet in Appendix C. Using this database, in conjunction with the calibrated 2DE Maps, unknown or unidentified proteins altered by chemical exposure can be more readily identified.

IPG-DALT. Improving the resolution of basic proteins. The representative 2DE Master Pattern (PHSDALT_1) generated by first-dimension pH-stabilized gel electrophoresis (IPG) is shown in (Fig. 5) in Appendix D. This figure illustrates a schematic map of the two-dimensional protein master-patterns of F344 male rat liver whole homogenate. By convention, acidic proteins are oriented to the left, basic to the right, low MW at the bottom, and high MW proteins toward the top of the pattern. Each circle or ellipse represents a single, detected protein. This master-pattern includes all proteins detected in all sample patterns and is thus a composite and not necessarily representative of any one sample pattern. Each circle or ellipse represents either a distinct protein or alternate forms of the same protein. Each protein spot is also arbitrarily assigned a master spot number (MSN). For comparison, the 2DE Master Pattern (F344LIVER_1) generated by conventional carrier-ampholyte isoelectric focusing and 2DE (ISO-DALT) is shown in Appendix A, Figure 1. Table 4, below, demonstrates the difference in protein resolution (# of spots resolved) between the two techniques. Although the IPG technique employed a broader pH gradient (pH 3-10), across the nine experimental groups, 22% fewer proteins were resolved (P<.002) using the first-dimension IPG method.

As a result of this experiment, it is clear that the Millipore pH-stabilized capillary gels are not a significant improvement over our present system with regard to the total number of proteins resolved. Despite a visible extension of the horizontal dimension toward the alkaline (right side), resolution of protein spots is poor and not analyzable. Additional investigation is required to reproducibly resolve the large number of protein spots with alkaline pI. Recently developed technology, now commercially available (ISOMORpH System, Large Scale Biology, Corp.), using multiple and reproducible IPG strip first-dimension separations may improve this technological barrier.

Table 4. Total number of matched spots

MASTERPATTERN	ISO-DALT	IPG-DALT
Liver_1	1239	1011
Liver_2	1459	1247
Liver_3	1273	1054
Liver_4	1258	1009
Liver_5	1242	936
Liver_6	1298	952
Liver_7	1181	886
Liver_8	1296	1006
Liver_9	1153	804
Mean ±SEM	**1267±21**	**989±40**

Investigation of Other Compounds and Target Tissues:

TCE effects on Mouse Liver 2D Patterns. A pilot study of mouse liver whole homogenates was conducted and the resulting mouse liver master pattern shown in Appendix E, Figure 6 was obtained. Although no specific protein identifications have been accomplished to date, statistical analysis of protein abundance variations with respect to TCE exposure level was conducted. The results of a two-tailed, unpaired Student t-test comparing 400, 800, and 1200 mg/kg exposures to a control group revealed dose-related alterations in the abundance of proteins resolved in the 2DE pattern. These results are shown in Table 5 below.

Table 5. Effect of TCE exposure on mouse liver protein abundance

Treatment	# of proteins altered
400 mg/kg, 60 days	20
800 mg/kg, 60 days	33
1200 mg/kg, 60 days	110

P<.001 *vs.* control , spots altered by exposure, either increased or decreased abundance

Proteins whose abundance was altered by TCE exposure can be assumed to have either increased or decreased as a result of the intoxication. Over 1,100 protein spots were resolved, thus a relatively small fraction of the complement of mouse liver proteins were actually effected by chronic exposure to TCE. Further analysis of these results will establish the identity of the proteins altered by this treatment and identify the nature of the TCE effect, *i.e.* upregulation, downregulation, or specific alterations in protein degradation and turnover. Nevertheless, these preliminary results demonstrate the capacity of the 2DE mapping approach in even the simplest analyses as a screening tool for toxicity testing. The 2DE map of mouse liver homogenate proteins also provides a basis for comparison to other species and sets the stage for similar comparisons to *in vitro* toxicologic applications.

Toxicity Experiments - ADN Effects on Rat Serum. Preliminary data obtained from rat serum gel patterns indicate the 2D pattern bears a strong resemblance to the well-characterized human serum pattern [26]. Our initial rat serum 2D master pattern is shown below in Appendix E, Figure 7. The pattern consists of over 600 protein spots, many of which exist as microheterogeneities or charge variants. This is the result of the high degree of glycosylation that characterizes many body fluid proteins. Statistical analysis of the protein pattern with respect to ammonium dinitramide exposure revealed a general lack of effect by any exposure level. Results shown in Table 6 document this effect.

Table 3. Effect of Ammonium Dinitramide exposure on Sprague-Dawley serum protein abundance

Treatment	# of proteins altered
20 mg/100ml , 90 days	2
100 mg/100ml, 90 days	2
200 mg/100ml, 90 days	4

P<.001 *vs.*control , spots altered by exposure, either increased or decreased abundance

The outcome of this analysis is not surprising given the lack of systemic effects observed in these same animals. It also emphasizes the stability of the 2D protein pattern across several groups of animals (n=5/group). The few proteins that were altered by these exposures correspond to alpha1-B glycoprotein (2 and 20 mg/100ml) in the human but are unidentified in the high-dose (200 mg/100ml) group. The quality of the gel patterns, the number of proteins resolved, and the potential extrapolation to/from human serum samples encourage the development of this aspect of pattern recognition studies. Serum samples (along with cerebrospinal fluid) are easily obtained from many animal models. Therefore, 2D patterns derived from these samples can increase the efficient use of animals in animal models and can credibly serve as a source of information regarding toxic effect, in addition to conventional systemic indices.

Effect of thioacetamide exposure on rat liver stress protein expression. Thioacetamide (TA) is a well known hepatotoxicant. It has been reported that an obligate intermediate of TA binds to proteins with the formation of acetylimidolysine derivatives that are responsible for TA-induced hepatotoxic effects. TA has also been reported to cause chemically-induced cell death via both apoptosis and necrosis. The objective of this study was two-fold. First, to investigate the effect of TA exposure on protein charge modifications in the rat liver and second, to study the role of these molecular correlates in the regulation of cell death. Male Sprague-Dawley rats (200-225 g, 7-8 wk old) were divided into 4 major groups and treated intraperitoneally with a 12-fold dose-range of TA (50, 150, 300 and 600 mg TA/kg) dissolved in water. The effect of TA administration on the 2DE protein pattern is shown in Appendix E, Figures 8-13. Figures 8-12 depict images of portions of stained-gel patterns representing various TA exposures where, with the exception of the vehicle-injected control, the charge-modifications are clearly evident. Even at the 50 mg/kg, 2 hr TA exposure, calreticulin, grp78, and ER60 already exhibit acidic charge variants. Visual inspection of these protein patterns suggests that the TA effect becomes more prominent with TA dose and time. One ER protein, grp94 (endoplasmin) and one cytosolic stress protein, hsp90, were poorly resolved by the separation technique thus preventing the quantitation of their charge modification. A subtle leftward "smearing" of the resolved spots at the higher TA doses suggests unresolved charge modification.

Quantification of the visible (Figs. 8-12) charge modification phenomena as CMI appears in Figure 13. CMI values relative to vehicle-injected control values were significantly altered in grp78, calreticulin, ER60, and PDI at the initial TA dose and time point as well as at all subsequent doses and time points. However, with the exception of PDI, at the 50 and 150 mg/kg doses, the elevation of CMI by TA generally appeared to reach a peak at 6 hr and then either level off or decline. In these same proteins, CMI was similarly elevated by the 300 and 600 mg/kg doses at 2-4 hr while after 6 hr of exposure or more, the rise in CMI appeared to continue. Hsc70 CMI was not significantly affected by TA administration until 6 hr after the 50 mg/kg dose. In fact, as the TA dose increased (300 & 600 mg/kg), hsc70 alterations were delayed until the 8 and 16 hr time points. In contrast, two hepatic stress proteins, hsp60 and grp75, were not altered by any TA exposure.

The effect of TA administration on rat liver cell death involves two distinct processes, *i.e.*, apoptosis and necrosis, whose onset is coincident with chemical exposure [27-28]. The predominance of one over the other seems to depend on TA dose, such that low doses favor cell death by apoptosis while high doses result in necrosis. This relationship is consistent with respect to tissue injury where moderate liver injury (as determined by serum alanine aminotransferase (ALT) activity) and subsequent recovery is

associated with low-dose TA exposure while severe, unrecoverable injury and subsequent death is a consequence of high dose exposure.

We have analyzed hepatic proteins by 2DE to investigate protein alterations associated with TA administration, alterations that might be related to and possibly indicative of the mechanisms regulating both response to injury and cell death. In this study, a set of specific stress proteins, whose 2DE coordinate positions have been identified previously [14] and whose cellular locations are known, was observed to undergo significant charge modifications as a result of TA administration. Furthermore, these charge modifications followed a dose-related pattern similar to the liver injury, apoptosis and necrosis observed using comparable models [27-28].

Calreticulin, grp78, PDI, and ER60, all prominent endoplasmic reticular (ER) proteins that play important roles in the disposition of cellular proteins [17, 29-30] underwent dose-related charge modification. The magnitude of the CMI alterations (up to 2.0) suggests protein adduct formation such as that implied by observations of the rat-specific hepatic carcinogen methapyrilene [3, 21, 31] where CMI alterations >1.0 were observed in the mitochondrial proteins hsp60 and grp75. The notion that the observed modifications are covalent protein adducts is further supported by the persistence of these charge changes despite the strongly dissociating conditions to which the proteins are subjected.

Though the exact nature of the protein modifications are as yet unconfirmed and covalent modification of other, less abundant hepatic proteins need to be examined, the present data suggest that TA is rapidly transformed by the ER-resident mixed-function oxidase system to its reactive sulfone metabolite(s) that covalently bind to the prominent ER proteins. This explains why the major proteins undergoing charge modification are ER resident. Not until later in the time-course does cytosolic protein adduct formation occur, made evident by the hsc70 CMI alterations. Hsc70 is a cytosolic chaperone [17] whose role includes mediating lysosomal degradation of intracellular proteins [32] and transport of proteins to mitochondria [33] and the nucleus [34]. Compared to the ER proteins, cytosolic hsc70's delayed charge modification suggests that the reactive metabolite(s) slowly leaks out of the ER at the low doses, and appears in the cytosol only at the latest time points in the high, 300 and 600 mg/kg doses. This notion is further supported by the absence, at any dose or time-point, of a TA-induced increase in CMI of mitochondrial chaperones hsp60 and grp75. As mentioned earlier, these proteins are selectively altered by methapyrilene, which targets the hepatic mitochondrion. In comparison, the present data suggest that TA has little or no detectable mitochondrial-specific toxicity at the time points studied.

Compartment-specific protein adduct formation as a consequence of chemical toxicity is not unusual, and is not restricted to mitochondria. Diclofenac (bioactivated to a reactive acyl glucuronide) causes protein adduct formation selectively in 60 and 80 kDa microsomal proteins both *in vitro* and *in vivo* [35] while the trifluoroacetylation of numerous proteins, microsomal and cytosolic, is widespread during halothane hepatitis [36].

Because the time-course of CMI alterations in ER proteins corresponds well with previously reported TA-induced cell injury, cell proliferation and cell death data [27-28], the question arises as to how these protein modifications are involved in the course of cell injury and cell death, if at all. Could the TA effect be related to the inactivation (by adduct formation) of various compartmental chaperones? Loss of chaperone/stress protein function has been shown to disrupt normal protein synthesis and maturation [37-38] and result in cell death [39]. We speculate that the charge modifications observed here may in some way be involved in the signaling of apoptosis and are somehow related to the recoverability of the liver from nonlethal TA doses (50-300 mg/kg) but not the lethal dose (600 mg/kg). Perhaps at the lethal dose,

and possibly at a threshold point beyond 300 mg/kg and 6 hr, irreversible protein modification results in a cascade of events signaling necrosis, hepatic failure and animal death.

Mangipudy [27] postulates that the high TA dose may inhibit the production of its reactive sulfone metabolite via substrate inhibition. This would explain the comparatively similar CMI values (at 2-6 hr) for 50 mg/kg and well as 300 or 600 mg/kg doses and the delayed CMI effects observed in ER and cytosolic proteins at the 300 and 600 mg /kg doses. These are interesting observations given their inconsistency with the paradigm that maintains high doses yield greater metabolic activation. The consequence of this substrate inhibition may prevent the onset of tissue repair mechanisms and lead to a rapid progression of tissue injury leading to hepatic failure and animal death.

The role of stress protein charge modifications induced by TA early in its assault on the liver tissue is unclear. However, the correspondence of the TA-induced charge modification time-course with the cell injury time course renders these proteins as excellent biomarkers of TA toxicity. Further study of these and other cellular proteins altered in a more expanded dose range and time-course may explain these effects and their connection to the switching from apoptotic cell death to necrosis.

CONCLUSION

We have addressed the second-year objectives originally set forth in the proposal and have exceeded our goals. The efficacy of large-scale two-dimensional electrophoresis combined with computerized image analysis of protein patterns is prominently demonstrated by the results presented in this report.

The development of a stress protein "fingerprint" is a major first step in the development of other, similarly recognizable patterns. The comprehensive database presented in this report also represents the groundwork of what will become a valuable resource for *comparing* toxic effects detected on a variety of 2D patterns and *predicting* (based on the cumulative observations accessible from the database) the effects of chemically similar compounds. The establishment of 2D master patterns for 1) rat liver, kidney, testis, brain, and serum and 2) mouse liver from *in vivo* experiments has now set the stage for the development of similar patterns derived from *in vitro* cell/tissue sources. Experiments using primary cell culture (hepatocytes and Hep G-2 cells) and tissue slices (from several organs and species) are forthcoming.

Finally, the assessment of pH stabilized gels led to the conclusion that while the alkaline pH range was somewhat extended, this improvement occurred at the cost of 20% of normally resolved proteins. Clearly another method must be developed. New technology is available, at considerable cost, which can solve this problem. Its implementation awaits additional funding.

LITERATURE CITED

[1] Anderson, N.L. (1991) *Two-dimensional Electrophoresis: Operation of the ISO-DALT System*, Large Scale Biology Press, Washington DC.

[2] Anderson, N. L., S.L. Nance, S.L. Tollaksen, F.A. Giere, & N.G. Anderson. (1985). *Electrophoresis* 6, 592-599.

[3] Anderson, N.L., D.C. Copple, R.A. Bendele, G.S. Probst, & F.C. Richardson. (1992). *Fund. Appl. Toxicol.* 18, 570-580.

[4] Yamazoe, Y., K. Nagata, S. Ozawa & R. Kato. (1994). *Chem.-Biol. Interact.* 92 107-117.

[5]   Matsui, M.,& H.K. Watanabe. (1982). *Biochem. J.* 204, 441-447.

[6]   Jones, A.L., R.C. Roberts & M.W. Coughtrie. (1993). *Biochem. J.* 296, 287-290.

[7]   Appel, R.D., J.C. Sanchez, A. Bairoch, O. Golaz, M. Miu, J.R. Vargas & D. Hochstrasser. (1993). *Electrophoresis* 14, 1232-1238.

[8]   Ozawa, S., K. Nagata, D. Gong, Y. Yamazoe & R. Kato. (1990). *Nucleic Acid Res.* 18, 4001.

[9]   Takahashi, M., H. Homma & M. Matsui. (1993). *Biochem. J.* 293, 795-800.

[10]   Iwasaki, K., Y. Tokuma, K. Noda & H. Noguchi. (1994). *Chem.-Biol. Interact.* 92, 209-217.

[11]   Ringer, D.P., T. Yerokun & A.S. Khan. (1994). *Chem.-Biol. Interact.* 92, 343-350.

[12]   Gong, D.-W., S. Ozawa, Y. Yamazoe & R. Kato. (1991). *J. Biochem.* 110, 226-231.

[13]   George, M.E. & M.E. Andersen. (1986). *Toxicol. Appl. Pharmacol.* 85, 169-180.

[14]   Witzmann, F.A., J.W. Clack, C.D. Fultz & B.M. Jarnot. (1995). *Electrophoresis* 16, 451-459.

[15]   Craig, E.A., B.D. Gambill, & R.J. Nelson. (1993). *Microbiol. Rev.* 57, 402-414.

[16]   Parsell, D.A. & S. Lundquist, (1993). *Annu. Rev. Genet.* 27, 437-496.

[17]   Morimoto, R.I., A. Tissières, & C. Georgopoulos, (1994). *The Biology of Heat Shock Proteins and Molecular Chaperones*, Cold Spring Harbor Laboratory Press, Cold Spring Harbor, NY.

[18]   Hendershot, L.M., J. Ting, & A.S. Lee. (1988). *Mol. Cell. Biol.* 8, 4250-4256.

[19]   Leno, G.H. & B.E. Ledford. (1990). *FEBS Lett.* 276, 29-33.

[20]   Leustek, T., D. Amir-Shapira, H. Toledo, N. Brot, & H. Weissbach. (1992). *Cell. Mol. Biol.* 38, 1-10.

[21]   Richardson, F.C., S.C. Strom, M. Copple, R.A. Bendele, G.S. Probst, & N.L. Anderson. (1993). *Electrophoresis* 14, 157-161.

[22]   Vanden Heuvel, J.P., B.I. Kuslikis, M.J. Van Rafelghem, & R.E. Peterson. (1991). *Toxicol. Appl. Pharmacol.* 107, 450-459.

[23]   Vanden Heuvel, J.P., B.I. Kuslikis, M.J. Van Rafelghem, & R.E. Peterson. (1991). *J. Biochem. Toxicol.* 6, 83-92.

[24]   Anderson, N.L. (1990). In: *New Horizons in Molecular Toxicology* (G.S. Probst, Ed.), pp. 65-71, FASEB, Bethesda MD.

[25]   Neidhardt, F.C., D.B. Appleby, P. Sankar, M.E. Hutton, & T.A. Phillips. (1989). *Electrophoresis* 10, 116-121.

[26]   Anderson, N.L. & N.G. Anderson. (1991). *Electrophoresis* 12, 883-906.

[27]   Mangipudy, R. S., S. Chanda, & H.M. Mehendale. (1995). *Environ. Health Perspec.* 103, 260-267.

[28]   Mangipudy, R. S., P.S. Rao, A. Warbritton, T.J. Bucci, & H.M. Mehendale. (1995). *The International Toxicologist.* 90-PF-9.

[29]   Nash, P. D., M. Opas, & M. Michalak. (1994). *Mol. Cell. Biochem.* 135, 71-78.

[30]   Urade, R. & M. Kito. (1992). *FEBS Lett.* 312, 83-86.

[31]   Cunningham, M.L., L.L. Pippin, N.L. Anderson, & M.L. Wenk. (1995). *Toxicol. Appl. Pharmacol.* 131, 216-223.

[32]   Chiang, H. -L., S.R. Terlecky, C.P. Plant, & J.F. Dice. (1989). *Science* 24, 382-385.

[33]   Sheffield, W. P., G.C. Shore, & S.K. Randall. (1990). *J. Biol. Chem.* 265, 11069-11076.

[34]   Shi, Y. & J.O. Thomas. (1992). *Molec. Cell. Biol.* 12, 2186-2192.

[35]   Kretz-Rommel, A. & U.A. Boelsterli. (1994). *Mol. Pharmacol.* 45, 237-244.

[36]   Pohl, L. R., D. Thomassen, N.R. Pumford, L.E. Butler, H. Satoh, V.J. Ferrans, A. Perrone, B.M. Martin, & J.L. Martin. (1991). *Adv. Exp. Med. Biol.* 283, 111-20.

[37]   Vogel, J. P., L.M. Misra, & M.D. Rose. (1990). *J. Cell. Biol.* 110, 1885-1895.

[38]   Kang, P. J., J. Ostermann, J. Shilling, W. Neupert, E.A. Craig, & N. Pfanner. (1990). *Nature (Lond.)* 348, 137-143.

[39]   Bruschi, S. A., K.A. West, J.W. Crabb, R.S. Gutta, & J.L. Stevens. (1993). *J. Biol. Chem.* 268, 23157-23161.

Appendix A

Figure 1. Schematic map of the two-dimensional protein master-pattern of F344 male rat liver whole homogenate. By convention, acid proteins are oriented to the left, basic to the right, low MW at the bottom, and high MW proteins toward the top of the pattern. Each circle or ellipse represents a single, detected protein. The horizontal dimension represents a pH gradient of 4-8. This master-pattern includes all proteins detected in each treatment group, and is thus a composite and not representative of any one sample pattern.

F344LIVER_1
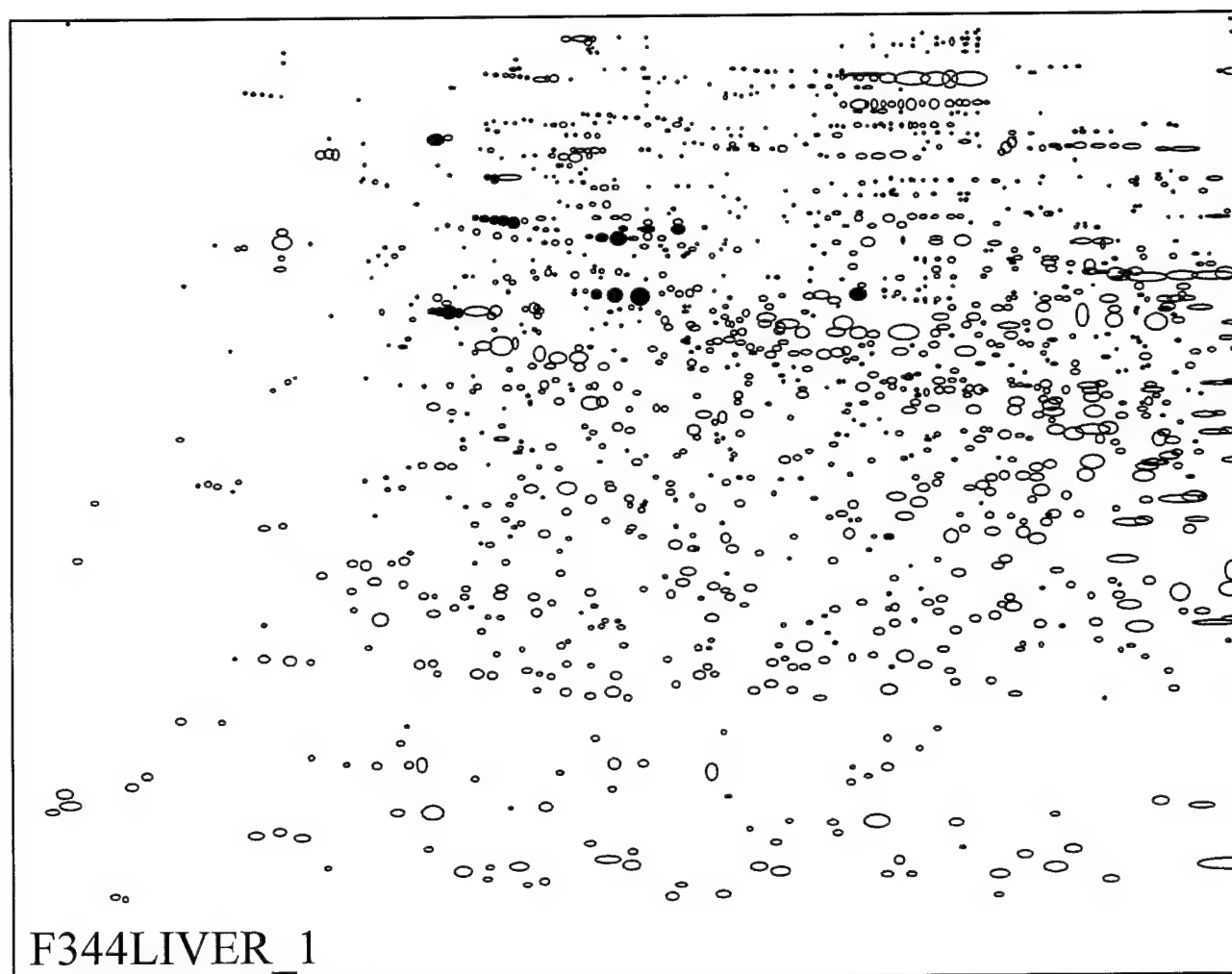
Figure 2. Postscript rendition of a TIFF image representing the F344 rat liver master pattern. The coordinates of the sulfotransferases studied are identified in the box area. Other, previously identified proteins are labeled for positional reference. As mentioned in the text, the ST's exist as microheterogeneities, small variations in protein charge and thus differential pI.
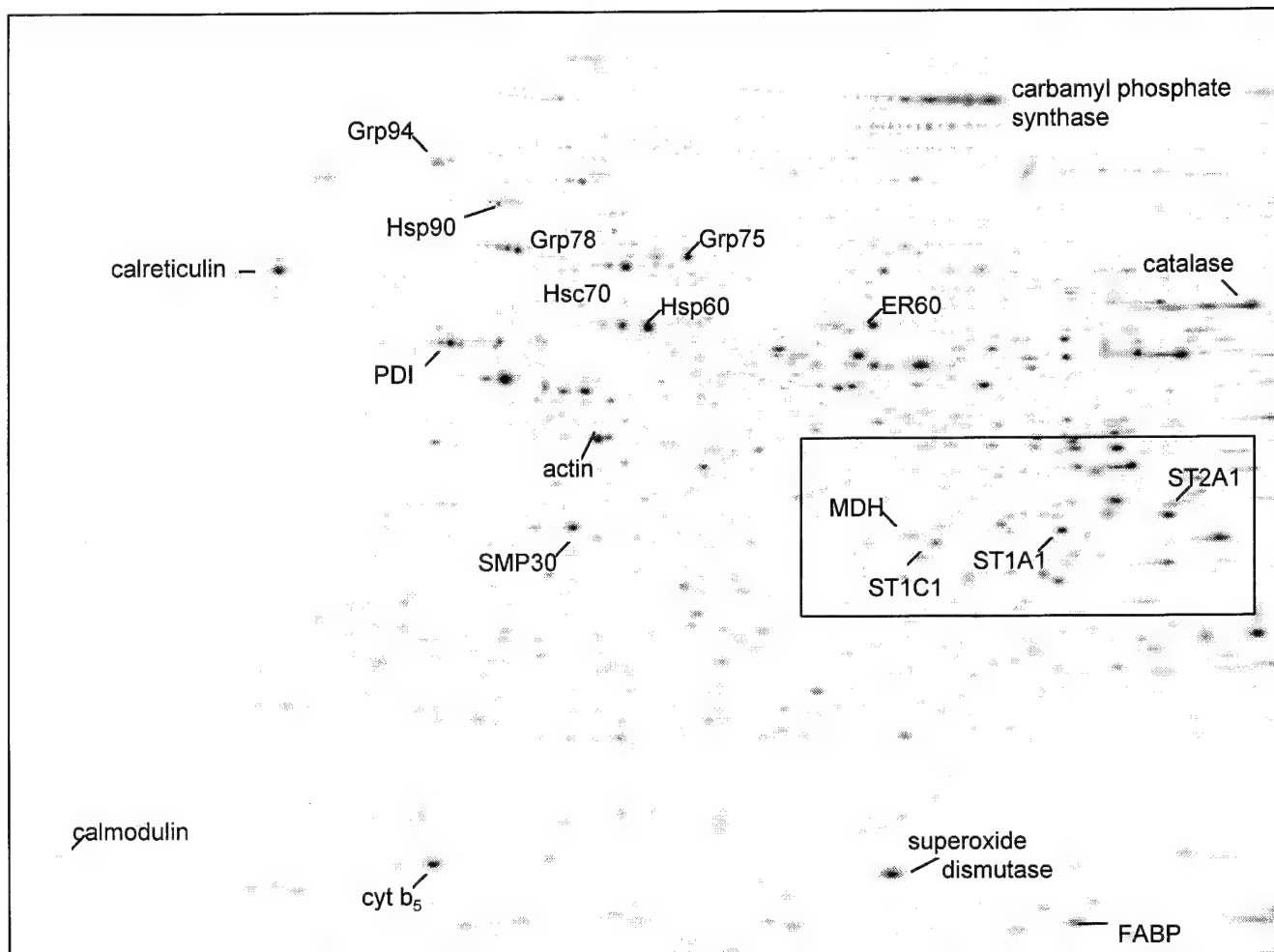
Figure 3. Comparison of the sum total of sulfotransferase protein abundance (mean ± SE) determined from the abundances of individual charge forms expressed in the liver (ANOVA, ST1A1 F=9.7, p<.0001; HAST-I F=25.4, p<.0001; * versus ad lib control and # versus pair-fed control (PFC) via SNK multiple-range test, p<.05). Abundances were calculated as described in the text (see Materials and Methods) based on the product of density (or amplitude), 2 , sx, and sy and have no units. Bars represent protein abundances for 150 mg PFOA/kg body weight (n=8), single injection, animals sacrificed on day 3 of exposure [PFOA], 2 mg (n=5) [PFDA2], 20 mg (n=5) [PFDA20], and 50 mg PFDA/kg body weight (n=9) [PFDA50/8], single injection, animals sacrificed on day 8 of exposure, 50 mg PFDA/kg body weight (n=5) [PFDA50/30], single injection, 30 days after exposure, clofibrate (ethyl- -p-chlorophenoxy-isobutyrate) 250 mg clofibrate/kg body weight, single intraperitoneal injection on each of 3 successive days, animals sacrificed on day five of exposure (n=10) [CLOF], and Di(2-ethylhexyl)phthalate, oral gavage, 1200 mg/kg per day, animals sacrificed on day 5 of exposure (n=3)[DEHP].
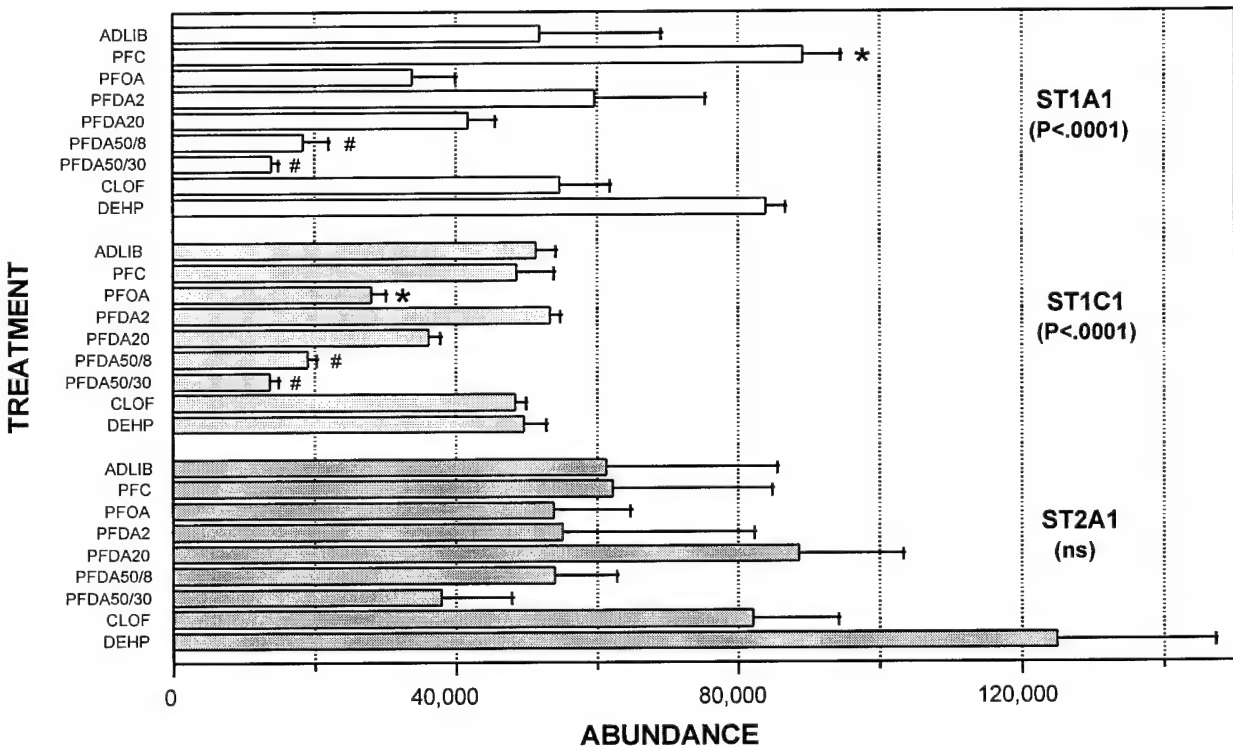
Figure 4. Schematic map of the two-dimensional protein master-pattern of F344 male rat kidney whole homogenate. By convention, acid proteins are oriented to the left, basic to the right, low MW at the bottom, and high MW proteins toward the top of the pattern. Each circle or ellipse represents a single, detected protein. The horizontal dimension represents a pH gradient of 4-8. This master-pattern includes all proteins detected in each treatment group, and is thus a composite and not representative of any one sample pattern.

F344KIDNEY_1

Table 2 Effects of peroxisome proliferator exposure on the abundance of various stress proteins detected in F344 rat liver and kidney whole homogenates, as % of ad lib group abundance

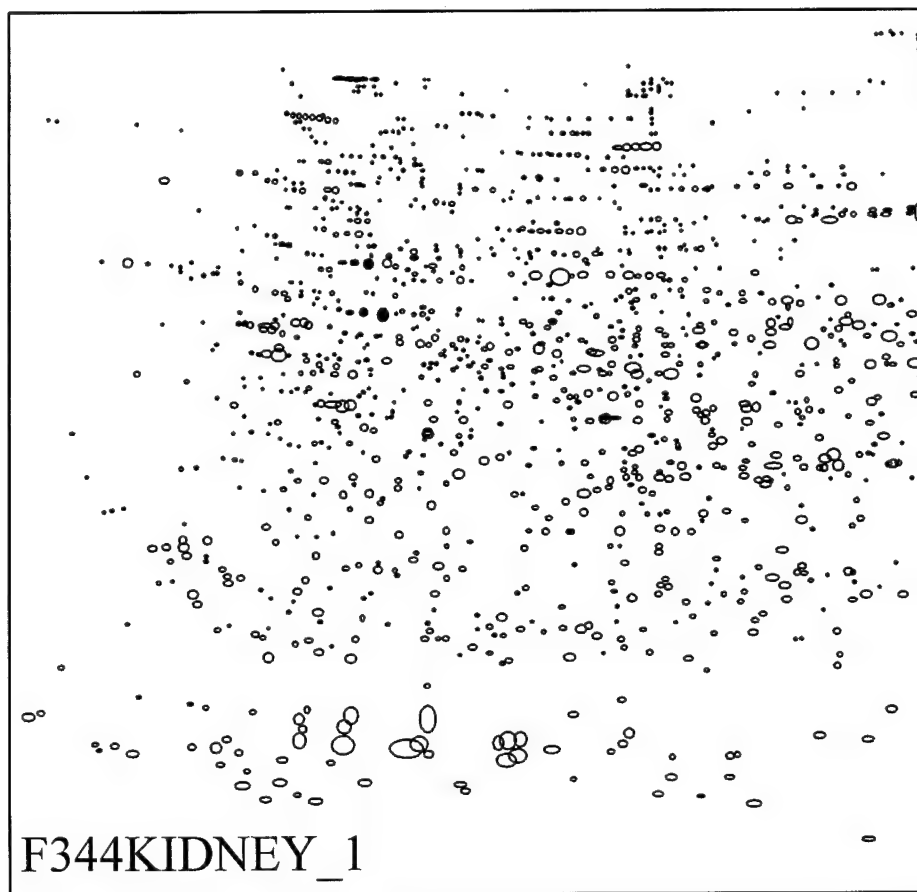| STRESS PROTEIN	Ad Lib	Pair-fed	PFOA 150mg/kg	PFDA 2mg/kg	PFDA 20mg/kg	PFDA 50mg/kg 8da	PFDA 50mg/kg 30da	Clofibrate	DEHP	F ratio	Prob.
Liver											
Hsp32	100	91	97	108	97	82	62‡	99	110	7.01	<0.0001
Hsp60	100	157¶	163¶	105	196‡	213‡	177¶	165¶	165¶	15.9	<0.0001
Hsc70	100	111	136¶	101	139¶	135¶	118	126	132	3.15	<0.0057
Hsp70	100	169¶	187¶	150¶	89	159¶	136	246‡	111	4.58	<0.0003
Hsp90	100	124	93	50	162¶	150	155	143	167	1.82	<0.0957
Grp75	100	147¶	155¶	119	210¶	302‡	216‡	151	151	20	<0.0001
Grp78	100	116	117	88	108	146¶	143¶	107	117	4.06	<0.0008
Grp94	100	118	98	78	103	95	75	105	122	0.978	<0.465
PDI	100	137	128	118	84	115‡	79‡	110	132	2.91	<0.0094
ER60	100	104	88	80	72	55‡	54‡	86	113	6.4	<0.0001
Kidney											
Hsp32	100	86¶	96	97	103‡	88	101‡	103‡	94	5.71	<0.0001
Hsp60	100	114	121	101	106	141‡	129	130¶	94	5.48	<0.0001
Hsc70	100	110	132¶	107	107	128¶	105	120	108	3.2	<0.0052
Hsp70	100	125	134‡	95	105	145‡	112	104	119	6.1	<0.0001
Hsp90	100	55	49	113	123	93	32	80	68	0.96	<0.459
Grp75	100	114	143‡	105	115	157‡	137	133‡	106	13.2	<0.0001
Grp78	100	92	111‡	100	94	87	88	96	103	3.53	<0.0026
Grp94	100	89	112	99	107	100	111	107	104	1.51	<0.179
PDI	100	95	118	96	97	101	103	94	112	0.87	<0.5481
ER60	100	96	116	113	118	127	113	103	121	0.444	<0.8885

‡ sig. diff. vs. pair-fed
¶ sig. diff. vs. adlib

Appendix B

F344LIVER_1   Master Pattern Database

MSN	Identification (name)	MW calc.	Y coord.	pI calc.	X coord.	Volume (ave. control)	VOL % of tot	Reference
75	catalase	59152	772.8	7.68	2974.9	89018	0.73%	comigration of purified form (Molec. Anat. Lab.)
67	catalase	58825	778.0	7.48	2868.5	111874	0.92%	comigration of purified form (Molec. Anat. Lab.)
185	lamin B	66260	674.0	4.98	1352.4	3330	0.03%	homologous position (Anderson et al., Electrophoresis, 1991)
394	carbamoyl phosphate synthase	165891	225.9	6.00	2032.2	3350	0.03%	homologous position (Anderson et al., Electrophoresis, 1991)
58	carbamoyl phosphate synthase	163645	229.4	6.13	2110.0	1397	0.01%	homologous position (Anderson et al., Electrophoresis, 1991)
374	cytochrome b5	17321	2247.6	4.48	922.8	8499	0.07%	homologous position (Anderson et al., Electrophoresis, 1991)
139	carbamoyl phosphate synthase	165203	227.0	6.07	2075.7	6488	0.05%	homologous position (Anderson et al., Electrophoresis, 1991)
96	cytochrome b5	17326	2247.3	4.57	1009.8	92948	0.77%	homologous position (Anderson et al., Electrophoresis, 1991)
48	actin (beta)	42857	1118.1	5.05	1406.3	97553	0.80%	homologous position (Anderson et al., Electrophoresis, 1991)
78	actin (gamma)	42971	1114.9	5.09	1433.5	28391	0.23%	homologous position (Anderson et al., Electrophoresis, 1991)
351	NADPH cytochrome P450 reductase	72213	607.0	5.13	1467.1	5472	0.05%	homologous position (Anderson et al., Electrophoresis, 1991)
122	NADPH cytochrome P450 reductase	72218	606.9	5.17	1494.8	10430	0.09%	homologous position (Anderson et al., Electrophoresis, 1991)
296	alpha-2u globulin	19121	2138.3	5.48	1702.7	56948	0.47%	homologous position (Anderson et al., Electrophoresis, 1991)
140	calmodulin	17708	2223.7	3.99	117.4	26965	0.22%	homologous position (Anderson et al., Electrophoresis, 1991)
1532	calmodulin	18246	2190.9	3.99	103.7	14421	0.12%	homologous position (Anderson et al., Electrophoresis, 1991)
688	apolipoprotein A-I	24745	1826.1	5.32	1594.6	3579	0.03%	homologous position (Anderson et al., Electrophoresis, 1991)
1545	apolipoprotein A-I	24326	1847.8	5.46	1693.7	11349	0.09%	homologous position (Anderson et al., Electrophoresis, 1991)
60	tubulin alpha	54317	855.2	4.86	1264.1	14328	0.12%	homologous position (Anderson et al., Electrophoresis, 1991)
124	tubulin alpha	53879	863.3	4.88	1279.0	13252	0.11%	homologous position (Anderson et al., Electrophoresis, 1991)
187	superoxide dismutase	16823	2278.6	6.13	2111.7	143464	1.18%	homologous position (Anderson et al., Electrophoresis, 1991)
287	superoxide dismutase	36308	1325.6	6.76	2476.1	37004	0.30%	homologous position (Anderson et al., Electrophoresis, 1991)
103	tubulin beta	53213	876.0	4.74	1160.2	11897	0.10%	homologous position (Anderson et al., Electrophoresis, 1991)
29	tubulin beta	53942	862.2	4.75	1170.0	30411	0.25%	homologous position (Anderson et al., Electrophoresis, 1991)
391	tubulin alpha	53180	876.7	4.88	1275.0	7388	0.06%	homologous position (Anderson et al., Electrophoresis, 1991)
494	tubulin alpha	54197	857.4	4.84	1244.0	6261	0.05%	homologous position (Anderson et al., Electrophoresis, 1991)
45	serum albumin precursor	65731	680.5	6.10	2094.5	59197	0.49%	homologous position (Anderson et al., Electrophoresis, 1991)
74	pro-albumin	65991	677.3	6.50	2327.9	59034	0.49%	homologous position (Anderson et al., Electrophoresis, 1991)
111	pyruvic acid carboxylase	129379	301.1	6.45	2297.0	12435	0.10%	homologous position (Anderson et al., Electrophoresis, 1991)
299	lamin B	66121	675.7	4.93	1318.6	2205	0.02%	homologous position (Anderson et al., Electrophoresis, 1991)
158	pro-albumin	65636	681.7	6.39	2262.0	9377	0.08%	homologous position (Anderson et al., Electrophoresis, 1991)
43	pyruvic acid carboxylase	128864	302.5	6.38	2258.9	3991	0.03%	homologous position (Anderson et al., Electrophoresis, 1991)
506	serum albumin precursor	65699	680.9	5.97	2016.3	10356	0.09%	homologous position (Anderson et al., Electrophoresis, 1991)
330	pyruvic acid carboxylase	129339	301.2	6.33	2229.8	1782	0.01%	homologous position (Anderson et al., Electrophoresis, 1991)
186	pyruvic acid carboxylase	129556	300.6	6.52	2337.3	7735	0.06%	homologous position (Anderson et al., Electrophoresis, 1991)
33	ATPase F1 beta (Mitcon:1)	49235	958.4	4.71	1139.2	29263	0.24%	homologous position (Anderson et al., Electrophoresis, 1991)
6	carbamoyl phosphate synthase	161516	232.9	6.39	2263.0	120304	0.99%	homologous position (Anderson et al., Electrophoresis, 1991)
3	carbamoyl phosphate synthase precursor	162068	232.0	6.29	2205.0	146476	1.21%	homologous position (Anderson et al., Electrophoresis, 1991)
152	ATPase F1 beta (Mitcon:1)	49480	953.0	4.81	1218.3	4242	0.03%	homologous position (Anderson et al., Electrophoresis, 1991)
7	carbamoyl phosphate synthase	161027	233.7	6.53	2347.0	160715	1.32%	homologous position (Anderson et al., Electrophoresis, 1991)
22	ATPase F1 beta (Mitcon:1)	49184	959.6	4.76	1183.9	136043	1.12%	homologous position (Anderson et al., Electrophoresis, 1991)
11	carbamoyl phosphate synthase precursor	160522	234.6	6.45	2298.7	15435	0.13%	homologous position (Anderson et al., Electrophoresis, 1991)
10	carbamoyl phosphate synthase	162948	230.6	6.19	2145.6	2416	0.02%	homologous position (Anderson et al., Electrophoresis, 1991)
80	enolase alpha	48186	982.2	6.51	2334.2	72386	0.60%	homologous position (LSB Corp., 1994)
256	F1 ATPase delta	23107	1912.3	6.18	2143.3	33515	0.28%	homologous position (LSB Corp., 1994)
134	arginase	40212	1196.1	7.14	2685.6	95058	0.78%	homologous position (LSB Corp., 1994)
165	23kDa morphine-binding protein	23059	1914.9	5.12	1458.5	49544	0.41%	homologous position (LSB Corp., 1994)

ID	Protein							Method
225	purine nucleoside phosphorylase	32218	1481.6	6.76	2475.9	21120	0.17%	homologous position (LSB Corp., 1994)
279	cytochrome c oxidase (polypeptide II)	27023	1712.7	4.44	882.2	22329	0.18%	homologous position (LSB Corp., 1994)
171	3-HA-3,4-DO	31524	1510.3	5.35	1614.6	18428	0.15%	homologous position (LSB Corp., 1995)
423	protein kinase C inhibitor 1	15338	2373.1	6.76	2476.8	16168	0.13%	homologous position (LSB Corp., 1995)
233	carbonic anhydrase III	28530	1641.7	7.70	2986.8	132817	1.09%	homologous position (LSB Corp., 1995)
166	hydroxyarylamine sulfotransferase	34353	1397.4	6.31	2218.7	43113	0.36%	homologous position (LSB Corp., 1995)
290	interferon-gamma induced protein	28779	1630.3	5.63	1801.6	16922	0.14%	homologous position (LSB Corp., 1995)
86	glutamate deydrog. (charge variant)	52058	898.8	7.17	2700.4	21944	0.18%	homologous position (LSB Corp., 1995)
220	malate dehydrogenase	34811	1380.2	6.22	2163.4	37664	0.31%	homologous position (LSB Corp., 1995)
77	glutamate dehydrogenase	51815	903.6	7.36	2804.3	202947	1.67%	homologous position (LSB Corp., 1995)
52	aldehyde dehydrogenase	50602	928.8	6.25	2182.2	125806	1.04%	homologous position (Pavlica et al., BBA, 1990)
558	3-hydroxy-3-methylglutaryl CoA synthase	72210	607.0	5.07	1418.3	1042	0.01%	immunologic (Anderson et al., Electrophoresis, 1991)
263	3-hydroxy-3-methylglutaryl CoA synthase	28304	1652.2	4.86	1263.3	7642	0.06%	immunologic (Anderson et al., Electrophoresis, 1991)
193	3-alpha-hydroxysteroid-dihydrodiol dehydrog.	36371	1323.3	7.04	2630.0	34376	0.28%	immunologic (Anderson et al., Electrophoresis, 1991)
2	calreticulin precursor	66594	669.8	4.23	642.2	81703	0.67%	immunologic (Anderson et al., Electrophoresis, 1991)
180	3-alpha-hydroxysteroid-dihydrodiol dehydrog.	36272	1326.9	7.30	2772.8	52499	0.43%	immunologic (Anderson et al., Electrophoresis, 1991)
505	calreticulin precursor	63181	713.9	4.23	640.6	3952	0.03%	immunologic (Anderson et al., Electrophoresis, 1991)
295	3-hydroxy-3-methylglutaryl CoA synthase	28834	1627.8	4.76	1183.2	5156	0.04%	immunologic (Anderson et al., Electrophoresis, 1991)
259	3-hydroxy-3-methylglutaryl CoA synthase	28388	1648.3	4.76	1179.7	7691	0.06%	immunologic (Anderson et al., Electrophoresis, 1991)
51	calreticulin precursor	68951	642.1	4.23	642.0	15293	0.13%	immunologic (Anderson et al., Electrophoresis, 1991)
369	3-hydroxy-3-methylglutaryl CoA synthase	54302	855.5	5.70	1849.4	6143	0.05%	immunologic (Anderson et al., Electrophoresis, 1991)
161	calreticulin precursor	61117	743.1	4.23	636.5	7321	0.06%	immunologic (Anderson et al., Electrophoresis, 1991)
192	tropomyosin (nonmuscle)	30570	1550.8	4.49	941.9	14667	0.12%	immunologic (LSB Corp., 1994)
44	cytokeratin	51859	902.8	6.00	2032.7	79495	0.66%	immunologic (LSB Corp., 1994)
35	cytokeratin	47753	992.3	5.01	1375.7	48254	0.40%	immunologic (LSB Corp., 1994)
36	ER60	56103	823.1	6.06	2068.4	84413	0.70%	immunologic (LSB Corp., 1994)
112	protein disulfide isomerase	53977	861.5	4.57	1014.5	7257	0.06%	immunologic (Mol. Anat. Lab via ab from StressGen)
275	protein disulfide isomerase	55117	840.6	4.61	1048.4	21670	0.18%	immunologic (Mol. Anat. Lab via ab from StressGen)
4	Grp94 (endoplasmin)	105085	385.2	4.61	1053.4	15428	0.13%	immunologic (Mol. Anat. Lab via ab from StressGen)
55	Hsp90	85613	493.3	4.72	1149.6	9042	0.07%	immunologic (Mol. Anat. Lab via ab from StressGen)
15	protein disulfide isomerase	53830	864.3	4.61	1053.6	67905	0.56%	immunologic (Mol. Anat. Lab via ab from StressGen)
26	Hsp60 (Mitcon:2)	56222	821.1	5.13	1465.5	40809	0.34%	immunologic (Mol. Anat. Lab via ab from StressGen)
50	Hsp60 (Mitcon:2)	56396	818.1	5.07	1419.5	7549	0.06%	immunologic (Mol. Anat. Lab via ab from StressGen)
12	Hsp90	85291	495.5	4.79	1202.3	25459	0.21%	immunologic (Mol. Anat. Lab via ab from StressGen)
40	protein disulfide isomerase	53885	863.2	4.59	1030.2	26170	0.22%	immunologic (Mol. Anat. Lab via ab from StressGen)
42	protein disulfide isomerase	53661	867.5	4.64	1077.5	17373	0.14%	immunologic (Mol. Anat. Lab via ab from StressGen)
106	Grp75 (Mitcon:3)	69336	637.8	5.16	1486.1	3398	0.03%	immunologic (Mol. Anat. Lab via ab from StressGen)
28	Grp75 (Mitcon:3)	69196	639.3	5.25	1547.5	16017	0.13%	immunologic (Mol. Anat. Lab via ab from StressGen)
20	Hsp60 (Mitcon:2)	55968	825.5	5.22	1527.9	114297	0.94%	immunologic (Mol. Anat. Lab via ab from StressGen)
116	Grp75 (Mitcon:3)	70868	621.0	5.36	1623.2	6664	0.05%	immunologic (Mol. Anat. Lab via ab from StressGen)
19	Grp75 (Mitcon:3)	69070	640.8	5.36	1623.4	48734	0.40%	immunologic (Mol. Anat. Lab via ab from StressGen)
32	Hsp90	84777	499.2	4.75	1167.6	14525	0.12%	immunologic (Mol. Anat. Lab via ab from StressGen)
1	Grp94 (endoplasmin)	103957	390.2	4.58	1021.7	57834	0.48%	immunologic (Mol. Anat. Lab via ab from StressGen)
176	PST-1; arylsulfotransferase	35195	1365.9	6.84	2519.5	70045	0.58%	immunologic (Molec. Anat. Lab. via ab from Coughtrie)
406	hydroxyarylamine ST (charge variant)	34226	1402.3	6.04	2056.1	10076	0.08%	immunologic (Molec. Anat. Lab. via ab from Coughtrie)
396	PST-1 (charge variant)	35105	1369.2	6.62	2394.6	10716	0.09%	immunologic (Molec. Anat. Lab. via ab from Coughtrie)
346	Hsp32??	29625	1592.2	6.48	2316.7	13879	0.11%	immunologic (Molec. Anat. Lab. via ab from StressGen)
385	Hsp32??	31984	1491.2	6.18	2142.9	14288	0.12%	immunologic (Molec. Anat. Lab. via ab from StressGen)
540	Hsp32??	24650	1831.0	5.92	1983.5	9152	0.08%	immunologic (Molec. Anat. Lab. via ab from StressGen)
309	fatty acid binding protein	14780	2409.4	6.90	2552.5	67573	0.56%	immunologic (Molec. Anat. Lab. via ab from StressGen)
776	Hsp70	65617	682.0	5.53	1737.6	1212	0.01%	immunologic (Molec. Anat. Lab. via ab from StressGen)
1537	Grp78/BiP	72356	605.5	4.69	1119.7	647	0.01%	immunologic (Witzmann et al., Fund. Appl. Tox., 1994)
1536	Grp78/BiP	72076	608.4	4.72	1142.2	5987	0.05%	immunologic (Witzmann et al., Fund. Appl. Tox., 1994)
18	Grp78/BiP	71751	611.7	4.74	1167.3	26304	0.22%	immunologic (Witzmann et al., Fund. Appl. Tox., 1994)

|								
14	Grp78/BiP	71465	614.7	4.77	1189.5	42583	0.35%	immunologic (Witzmann et al., Fund. Appl. Tox., 1994)
5	Grp78/BiP	70965	620.0	4.80	1214.3	64302	0.53%	immunologic (Witzmann et al., Fund. Appl. Tox., 1994)
24	Hsp73 (Hsc73) constitutive in unstressed	67215	662.3	5.09	1433.5	31112	0.26%	immunologic (xreact with antHsp70 from StressGen)
9	Hsp73 (Hsc73) constitutive in unstressed	66981	665.1	5.14	1474.0	89645	0.74%	immunologic (xreact with antHsp70 from StressGen)
130	Hsp73 (Hsc73) constitutive in unstressed	67475	659.2	5.04	1401.8	4713	0.04%	immunologic (xreact with antHsp70 from StressGen)
141	senescence marker protein (SMP30)	35546	1353.0	4.85	1256.6	23626	0.19%	sequence from gel spot (Meheus, Innogenetics)
76	laminin receptor protein	42585	1125.8	4.57	1015.6	22461	0.19%	sequence from gel spot (Meheus, Innogenetics)
62	senescence marker protein (SMP30)	35560	1352.5	4.97	1346.0	111435	0.92%	sequence from gel spot (Meheus, Innogenetics)

Appendix C

MSN	PROT ID	PROT NAMES	DB/NAME	EC NUMBER	SUBCELLULAR	COMMENTS	DB Aa	DB MW
	acetyl-CoA C-acetyltransferase	acetoacetyl-CoA thiolase	JU0072	2.3.1.9	mitochondria	rat liver: The enzyme plays a major	394	41,317
	acetyl-CoA C-acyltransferase	3-ketoacyl-CoA thiolase	A29452	2.3.1.16	mitochondria	rat liver	397	41,871
	acetyl-CoA C-acyltransferase	3-ketoacyl-CoA thiolase\ beta-ketothiolase\	B29452	2.3.1.16	peroxisome	rat liver	424	43,920
	acetyl-CoA C-acyltransferase A prec	3-ketoacyl-CoA thiolase\ beta-ketothiolase\	A35725\ JS039	2.3.1.16	peroxisome	rat liver	434	44,839
	acetyl-CoA C-acyltransferase B prec	3-ketoacyl-CoA thiolase\ beta-ketothiolase\	B35725\ A2932	2.3.1.16	peroxisome	rat liver; CoASH-initiated thiolysis of	424	43,820
	acetylcholinesterase precursor		JH0314\ S1568	3.1.1.7		rat	614	68,168
	acid phosphatase precursor		A33395	3.1.3.2		rat liver	423	48,319
	acid phosphatase precursor, prostatic		JH0152	3.1.3.2		rat	381	43,850
	acidic fibroblast growth factor		D37360			mouse	155	17,417
	acidic ribosomal protein P2 - rat	ribosomal phosphoprotein P2\ ribosomal pr	S22320; A02777		cytosolic	rat liver	115	11,692
	acrosin precursor		A37344	3.4.21.10	serine proteinase	mouse	418	46,816
	actin A(X)		A31900			mouse	375	41,693
	actin alpha, vascular smooth muscle (clone pM alpha VSM-2)		S02135		cDNA/mRNA	mouse	377	42,009
	actin beta		A38571		cytoskeletal	rat	375	41,750
	actin gamma, cytoskeletal		S11222		cDNA/mRNA	rat	375	41,792
	actin gamma, smooth muscle		A32788		mRNA (germ cells)	mouse (male)	376	41,877
	actin, skeletal muscle		A24904		DNA	mouse	377	42,051
	actin, smooth muscle		A31375		cDNA/mRNA	rat	376	41,877
	actin-associated protein p27		A60598		cytoskeleton	mouse	201	22,491
	actin-capping protein gCap39		A39834		mRNA	mouse	352	39,240
	activin receptor precursor		A39896		transmembrane serine	mouse	513	57,889
	acyl-CoA dehydrogenase	acyl dehydrogenase, medium-chain-specifi	A28436	1.3.99.3		rat liver	421	46,555
	acyl-CoA oxidase I chain A	A chain is cleaved to B and C chains; minus	A29328	1.3.3.6	peroxisome	rat liver	658	74,678
	acyl-CoA oxidase I chain B	aa chain 1-438	A29328	1.3.3.6	peroxisome	rat liver	438	
	acyl-CoA oxidase I chain C	aa chain 439-659	A29328	1.3.3.6	peroxisome	rat liver	220	
	acyl-CoA oxidase II chain A	A chain is cleaved to B and C chains; minus	B29328	1.3.3.6	peroxisome	rat liver	658	74,690
	acyl-CoA oxidase II chain B	aa chain 1-438	B29328	1.3.3.6	peroxisome	rat liver	438	
	acyl-CoA oxidase II chain C	aa chain 439-659	B29328	1.3.3.6	peroxidsome	rat liver	220	
	acylaminoacyl-peptidase	acyl-peptide hydrolase\ acylamino-acid-rele	A33706\ S0762	3.4.19.1		rat liver	732	81,383
	adenosylmethionine decarboxylase		JS0733	4.1.1.50	lyase	mouse	334	38,272
	adenosylmethionine decarboxylase	alpha chain	JQ0439\ B3178	4.1.1.50		essential step in spermidine biosynt	67	
	adenosylmethionine decarboxylase	beta chain	JQ0439\ B3178	4.1.1.50		essential step in spermidine biosynt	266	
	adipocyte lipid-binding protein		A30810			mouse	131	14,519
	adipocyte lipid-binding protein	adipocyte P2 protein\ myelin P2 protein hom	B25952\ PC1249		lipid binding	mouse	132	14,692
	adipocyte P2 protein		A24884			mouse	132	14,637
	adipocyte p27 protein		A28053			mouse	244	25,958
	adipose differentiation-related protein		S27864			mouse	425	46,664
	Ah receptor		JQ1485		transcription reguation	mouse	805	90,380
	albumin	serum albumin	A93872\ A92211\ A91946\ A919		plasma	rat plasma	583	
	alcohol dehydrogenase		A26468	1.1.1.1		rat liver	376	39,645
	alcohol dehydrogenase 2	alcohol dehydrogenase class III; ADH-2	S00331\ S0261	1.1.1.1		rat liver	373	39,426
	alcohol dehydrogenase class I		A33372	1.1.1.1		rat	376	39,645
	alcohol sulfotransferase		A33569	2.8.2.2		rat liver	284	33,080
	alcohol sulfotransferase a	alcohol sulfotransferase a	A34822	2.8.2.2		rat liver	284	33,251
	aldehyde dehydrogenase (NAD+)		S03564	1.2.1.3	mitochondria	rat liver	519	56,488
	aldehyde dehydrogenase (NAD+),	phenobarbital-inducible	A32616	1.2.1.3		rat	501	54,559

-2 Lys	-1 Lys	unshifted	+1 Lys	Δcharge	Calc Aa	Calc MW	N-*	Tyr	Trp	Val	Thr	Ser	Arg	Gln	Pro	Asn	Met	Leu	Lys	Ile	His	Gly	Phe	Glu	Asp	Cys	Ala	C-D	C-G
7.45	8.09	8.40	8.59	1	394	41,317	A	9	2	39	21	23	9	12	19	15	14	27	33	25	6	37	8	23	16	5	51	0	0
6.79	7.44	8.06	8.36	1	396	41,692	A	8	2	31	24	27	17	17	17	13	9	36	23	19	7	44	13	19	19	7	44	0	0
8.04	8.37	8.57	8.73	0	398	41,172	S	6	0	33	20	29	24	16	21	15	8	34	17	22	2	46	10	20	17	8	50	0	0
7.13	8.03	8.36	8.56	1	398	41,075	S	6	0	34	20	31	23	15	21	14	8	34	17	23	2	46	10	19	18	8	49	0	0
7.23	8.04	8.36	8.56	1	398	41,072	S	6	0	33	20	29	23	16	21	14	8	34	17	23	2	47	10	20	17	8	50	0	0
5.74	5.82	5.91	6.00	0	613	67,960	R	22	17	46	29	38	42	25	50	18	8	69	11	15	14	54	31	31	31	7	54	0	0
5.86	5.96	6.06	6.17	0	422	48,133	A	15	8	24	25	19	19	36	30	16	12	58	14	13	14	21	21	21	18	8	30	0	0
5.97	6.10	6.24	6.40	0	380	43,669	R	18	7	14	24	28	20	18	25	13	10	56	19	14	10	22	17	26	17	6	16	0	0
5.73	5.97	6.25	6.63	0	154	17,267	A	8	1	4	12	9	7	6	7	8	1	19	11	5	5	15	6	13	6	3	8	1	0
4.15	4.23	4.32	4.40	0	115	11,679	M	2	0	8	0	11	2	1	5	5	2	8	10	6	5	12	2	11	10	0	20	0	0
9.62	9.65	9.69	9.72	0	417	46,631	L	15	11	28	30	28	29	15	44	14	8	35	19	17	17	27	13	12	13	13	29	0	0
5.07	5.14	5.21	5.29	0	374	41,515	D	15	4	22	26	25	17	12	19	9	16	28	19	28	9	28	13	26	23	6	29	0	0
5.10	5.17	5.24	5.31	0	376	41,830	W	16	4	20	24	26	18	11	19	12	15	27	19	30	9	28	12	29	21	7	29	0	0
5.14	5.21	5.29	5.38	0	374	41,572	D	15	4	22	26	25	18	12	19	9	16	27	19	28	9	27	13	26	23	6	30	0	0
5.16	5.23	5.31	5.39	0	374	41,614	E	15	4	21	26	25	18	12	19	9	16	27	19	29	9	28	13	29	20	6	29	0	0
5.16	5.23	5.31	5.39	0	375	41,698	C	16	4	20	25	25	18	10	20	12	15	27	19	30	9	28	12	29	20	7	29	0	0
5.09	5.16	5.23	5.31	0	376	41,872	C	16	4	21	27	23	18	11	19	12	16	26	19	30	9	28	12	28	22	6	29	0	0
5.09	5.16	5.23	5.31	0	376	41,829	M	16	4	20	25	25	18	10	20	12	16	27	19	30	9	28	12	29	20	7	29	0	0
6.24	7.29	8.51	8.83	1	200	22,334	A	7	3	17	6	12	10	14	10	8	9	14	17	7	2	20	6	14	11	1	12	0	0
6.29	6.51	6.79	7.23	0	351	39,065	Y	9	6	17	12	24	21	21	21	15	4	29	21	21	8	28	15	25	18	5	31	0	0
5.47	5.54	5.61	5.68	0	512	57,692	G	17	11	35	24	37	22	18	30	20	15	46	31	29	14	32	20	38	28	19	38	0	0
6.55	7.07	7.68	8.10	1	396	43,635	K	15	4	20	24	21	19	19	17	13	10	27	30	28	4	38	18	31	17	6	42	0	1
8.22	8.40	8.53	8.63	0	658	74,265	M	30	8	42	45	38	32	33	31	30	20	67	40	37	18	44	24	43	24	7	45	0	0
6.68	6.99	7.54	8.08	0	438	49,638	M	21	5	19	37	22	22	21	24	20	17	38	24	28	11	32	19	32	13	5	28	0	0
8.47	8.77	8.96	9.10	0	221	24,732	Y	9	3	23	8	17	10	12	7	10	3	29	16	9	7	12	5	11	11	2	17	0	0
7.24	7.61	7.98	8.23	0	658	74,277	M	28	8	41	45	37	33	31	32	29	20	68	38	35	22	44	25	44	25	7	46	0	0
6.34	6.47	6.62	6.82	0	438	49,650	M	19	5	18	37	21	23	19	25	19	17	39	22	26	15	32	20	33	14	5	29	0	0
8.47	8.77	8.96	9.10	0	220	24,645	Y	9	3	23	8	16	10	12	7	10	3	29	16	9	7	12	5	11	11	2	17	0	0
5.36	5.41	5.46	5.52	0	731	81,160	E	24	16	61	29	67	34	35	50	18	18	75	30	24	19	54	29	45	39	19	45	0	0
5.39	5.54	5.71	5.92	0	333	38,098	E	13	4	20	21	35	15	20	14	11	10	27	21	16	4	16	25	18	22	7	14	0	0
4.33	4.48	4.63	4.81	0	66	7,496	E	1	2	5	4	8	3	5	1	0	0	6	4	3	1	3	3	7	5	1	4	0	0
5.98	6.40	7.28	8.09	0	266	30,471	S	12	2	15	17	26	12	14	13	12	10	22	17	13	3	14	21	11	17	6	9	0	0
6.43	7.89	8.55	8.87	1	131	14,502	C	2	2	16	11	9	7	2	1	4	4	6	14	8	0	11	6	8	11	2	7	0	0
6.44	7.89	8.55	8.87	1	131	14,544	C	2	2	17	11	9	7	2	1	4	4	6	14	8	0	10	6	8	11	2	7	0	0
6.43	7.89	8.55	8.87	1	131	14,489	C	2	2	16	12	9	7	2	1	3	4	6	14	8	0	11	6	8	11	2	7	0	0
8.57	8.89	9.10	9.25	0	243	25,797	K	2	1	30	14	21	12	3	10	11	9	24	15	10	4	20	9	10	13	2	23	0	0
5.90	6.06	6.24	6.47	0	424	46,480	A	13	3	47	30	41	14	31	13	18	14	32	30	15	7	20	8	27	19	5	37	0	0
5.87	5.93	5.99	6.05	0	804	90,148	S	23	7	33	38	76	40	72	60	32	15	80	33	36	23	40	39	39	46	17	55	0	0
5.67	5.73	5.80	5.87	0	584	65,829	E	21	1	35	33	24	24	25	30	20	6	56	53	13	15	17	26	57	32	35	61	0	1
8.26	8.40	8.52	8.61	0	375	39,468	S	3	2	36	24	27	9	9	23	6	5	30	31	24	9	35	18	15	19	16	34	0	0
6.38	6.72	7.28	7.82	0	373	39,381	A	5	4	37	23	25	9	9	16	10	7	22	30	28	6	41	16	23	15	14	33	0	0
8.26	8.40	8.52	8.61	0	375	39,468	S	3	2	36	24	27	9	9	23	6	5	29	31	25	9	35	18	15	19	16	34	0	0
7.29	8.02	8.37	8.58	1	283	32,911	P	12	12	17	15	20	6	7	13	10	11	29	29	16	5	19	18	15	18	3	8	0	0
6.56	7.33	8.03	8.36	1	283	33,082	P	13	11	14	17	15	7	6	17	11	11	30	28	17	4	18	19	17	17	3	8	0	0
5.37	5.47	5.58	5.70	0	500	54,306	S	18	7	46	26	25	18	26	24	20	9	34	31	23	6	46	24	27	28	9	53	0	0
6.38	6.59	6.90	7.42	0	500	54,366	S	11	7	39	25	32	17	20	23	20	11	35	38	35	9	45	23	32	23	9	46	0	0

Appendix D

Figure 5. This figure illustrates a schematic map of the two-dimensional protein master-pattern of F344 male rat liver whole homogenate. By convention, acidic proteins are oriented to the left, basic to the right, low MW at the bottom, and high MW proteins toward the top of the pattern. For comparison, the 2DE Master Pattern (F344LIVER_1) generated by conventional carrier-ampholyte isoelectric focusing and 2DE (ISO-DALT) is shown in Appendix A, Figure 1


PHSDALTLIVER_1
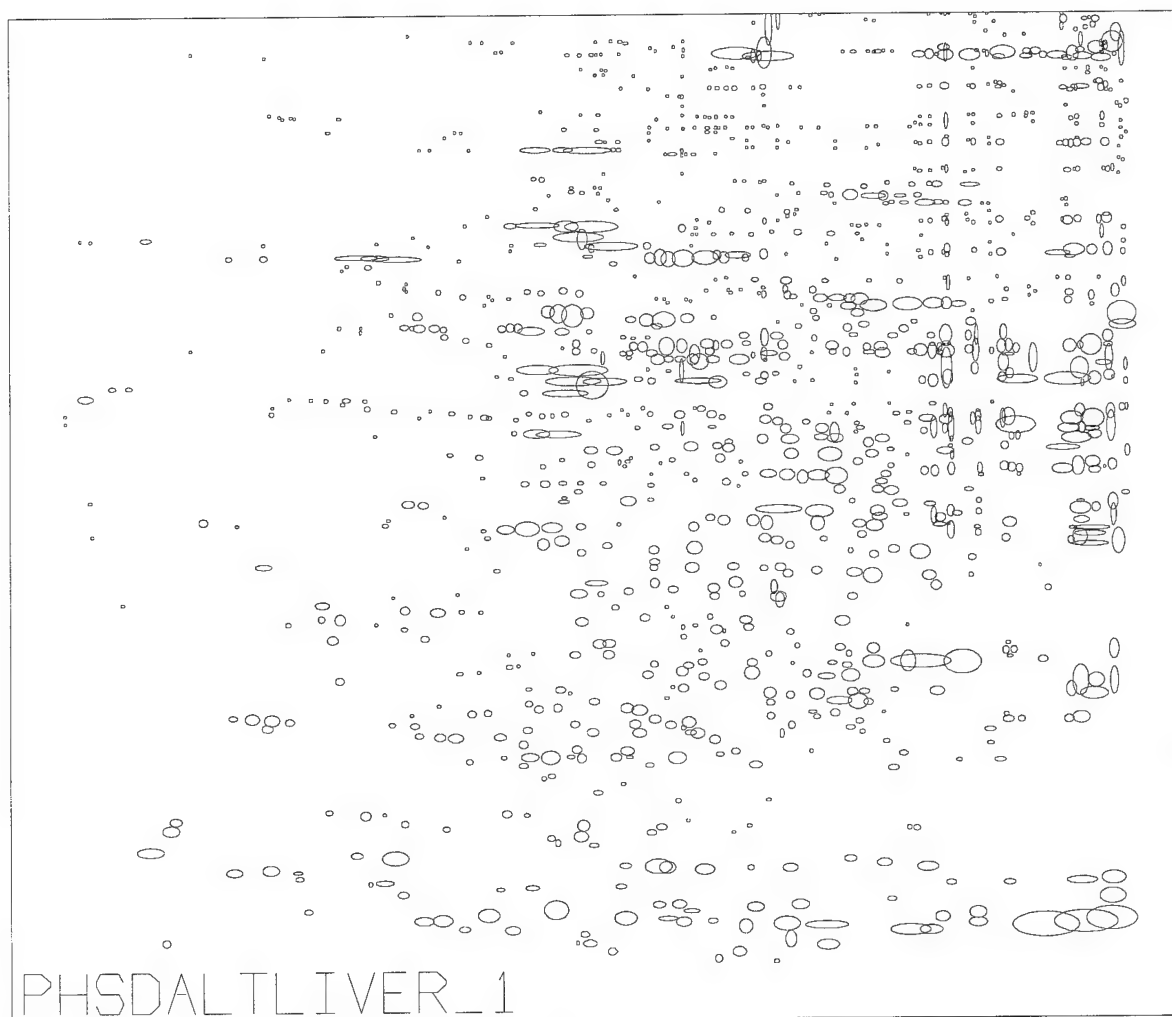
F344 Rat Liver - Millipore IPG-DALT
Experiment MILLIPORE

09:42 22-APR-95

Appendix E

Figure 6. This figure illustrates a schematic map of the two-dimensional protein master-pattern of the male B6C3F1 mouse liver whole homogenate. By convention, acidic proteins are oriented to the left, basic to the right, low MW at the bottom, and high MW proteins toward the top of the pattern. This master-pattern includes all proteins detected in all sample patterns and is thus a composite and not necessarily representative of any one sample pattern. Each circle or ellipse represents either a distinct protein or alternate forms of the same protein.

MOUSELIVER_1
B6C31 MALE MOUSE LIVER
Experiment TCE_GAVAGE   15:39 21-APR-95
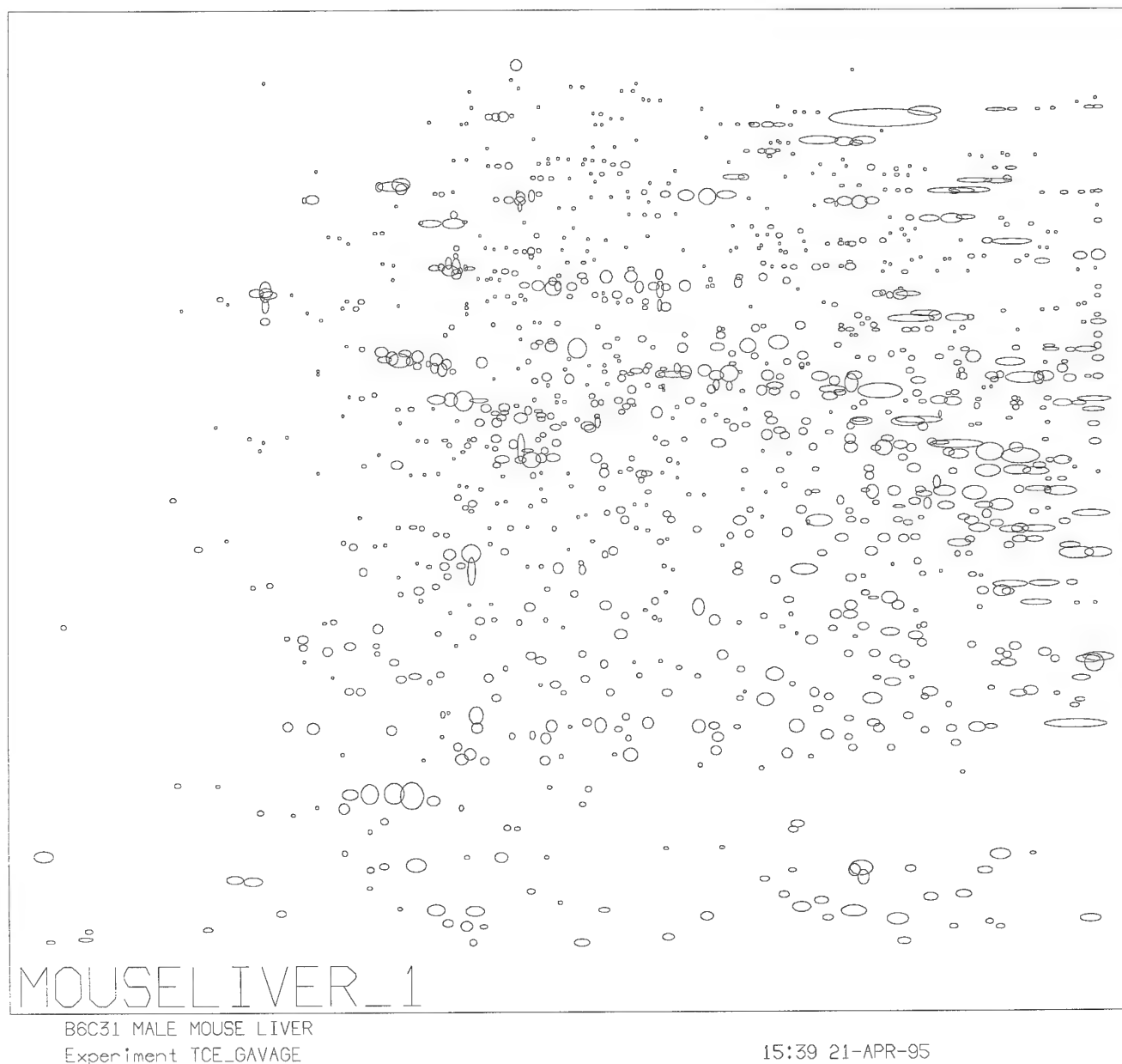
Figure 7. This figure illustrates a schematic map of the two-dimensional protein master-pattern of the male Sprague-Dawley rat serum. Map characteristics as in previous master patterns.

SDSERUM_1

SPRAGUE-DAWLEY RAT SERUM
Experiment DS_SERUM

14:32 21-APR-95
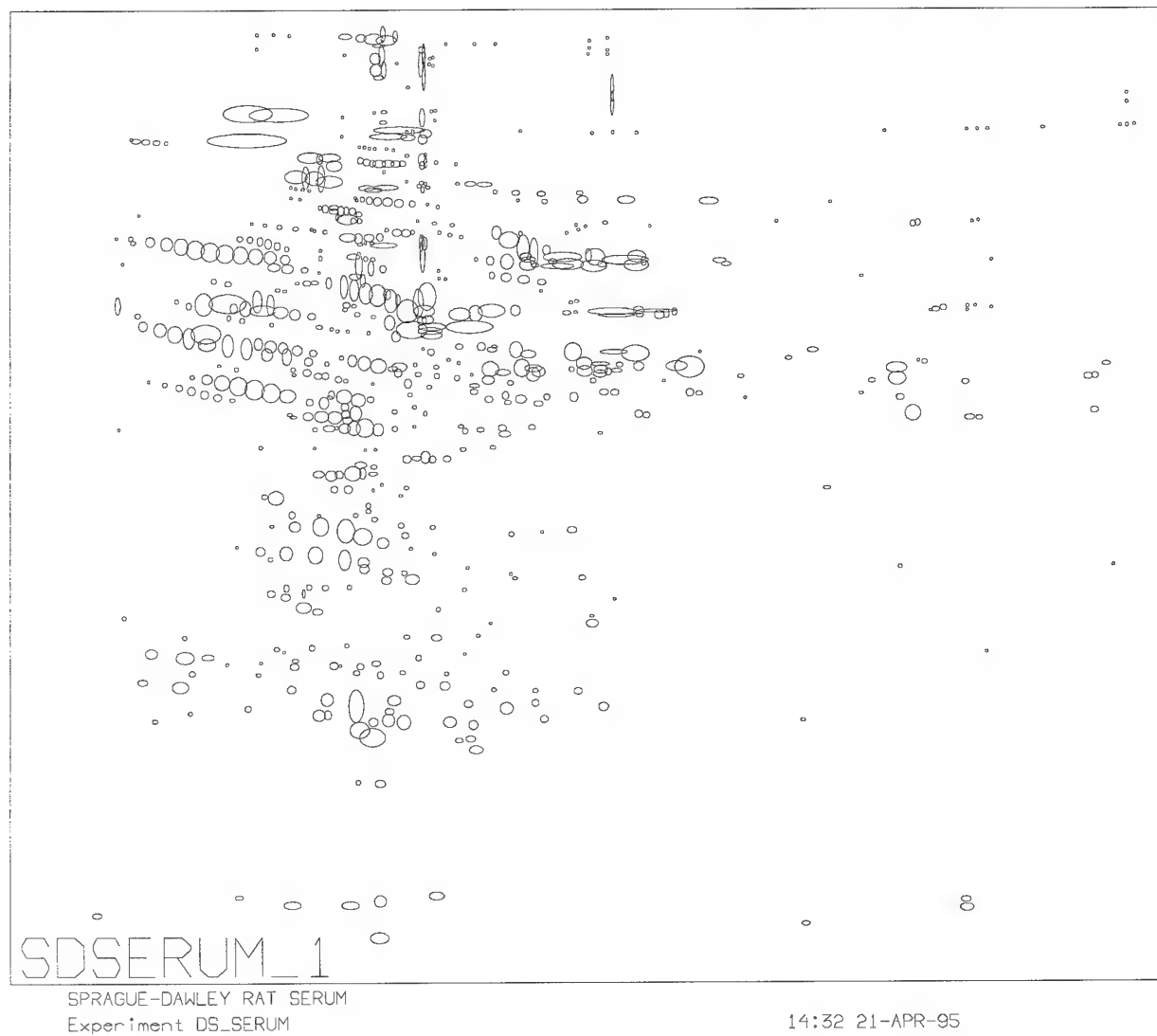
Figures 8 & 9. These figures illustrate representative gel patterns of a portion of the 2DE pattern of Sprague-Dawley liver homogenate containing the proteins studied. Actin and SMP30 (previously identified) are labeled for positional reference.


Vehicle-injected Control

TA 50 mg/kg, 2 hr
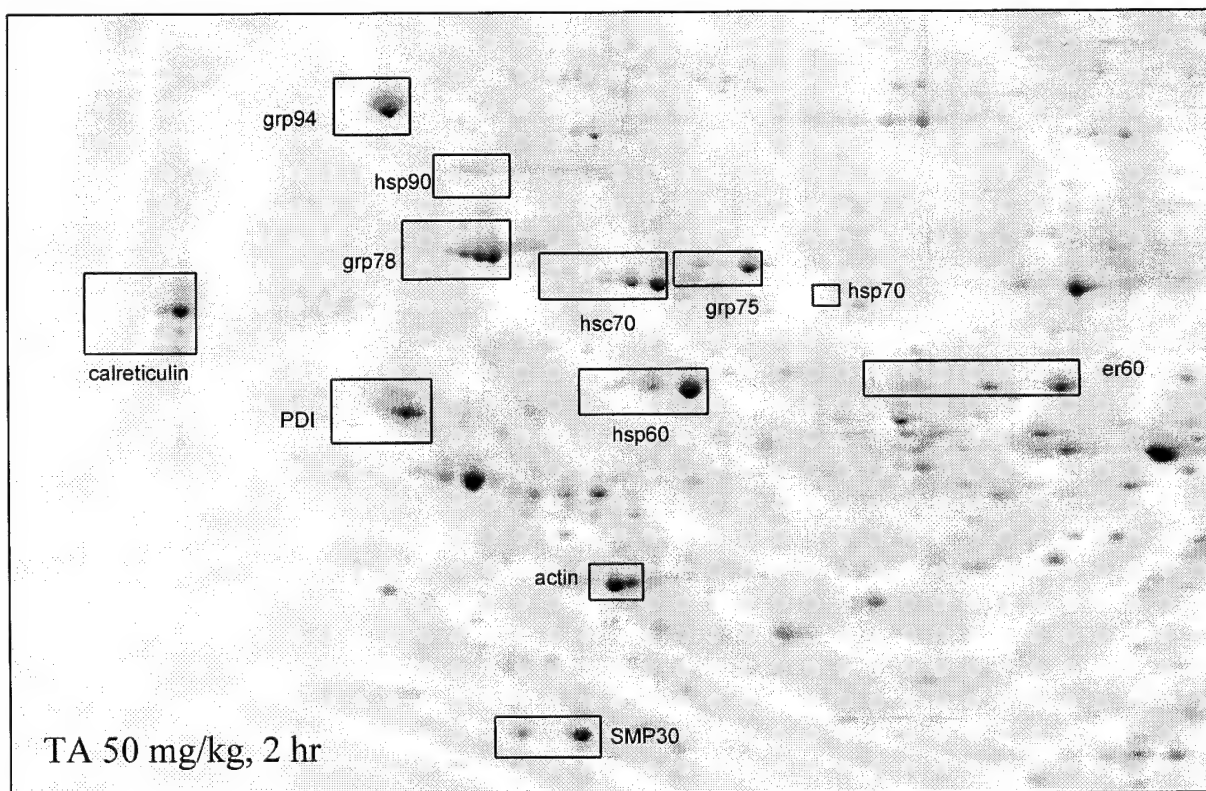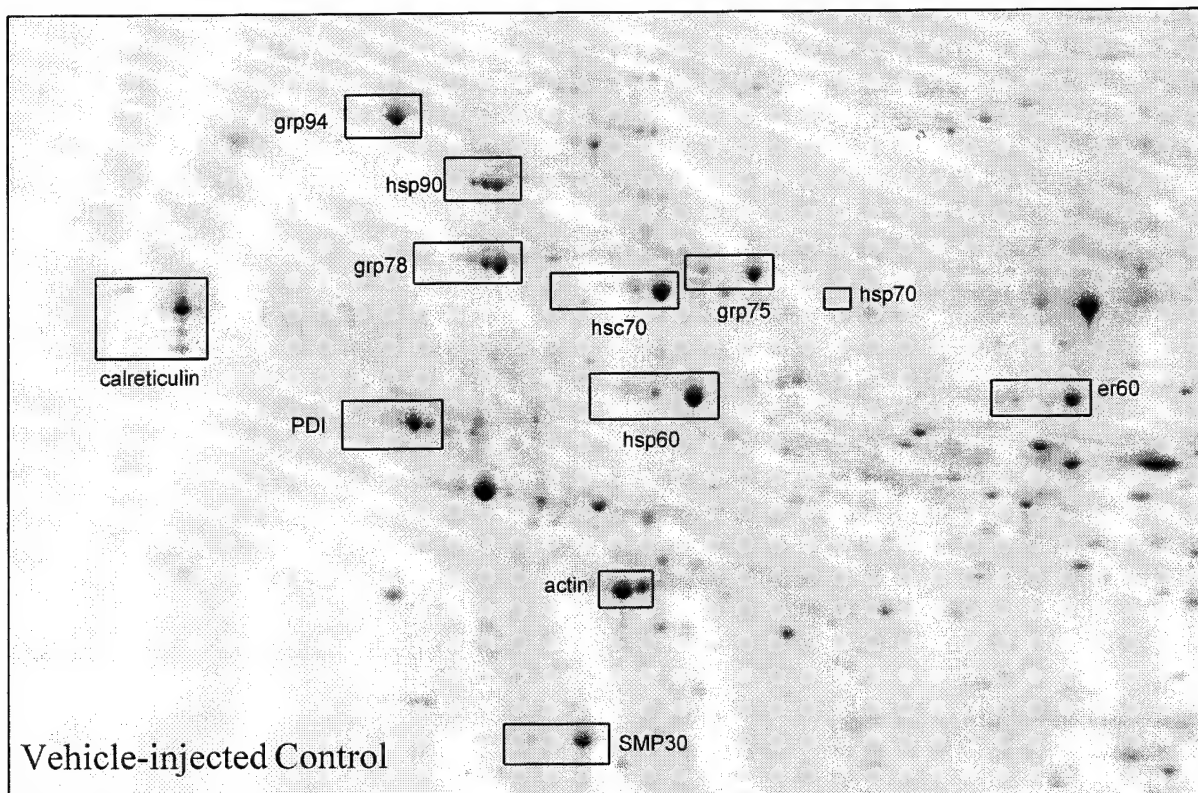
Figures 10 & 11. These figures illustrate gel patterns of Sprague-Dawley liver homogenate containing the proteins studied. The patterns depicted in these figures were obtained from the liver of a rat treated with 50 mg/kg TA for 2 hr and with 150 mg/kg TA for 6 hr. Note the the increasing appearance of charge variants (leftward appearing spots) for calreticulin, grp78 and ER60, hsc70 and PDI.

TA 150 mg/kg, 6hr

TA 600 mg/kg, 4hr
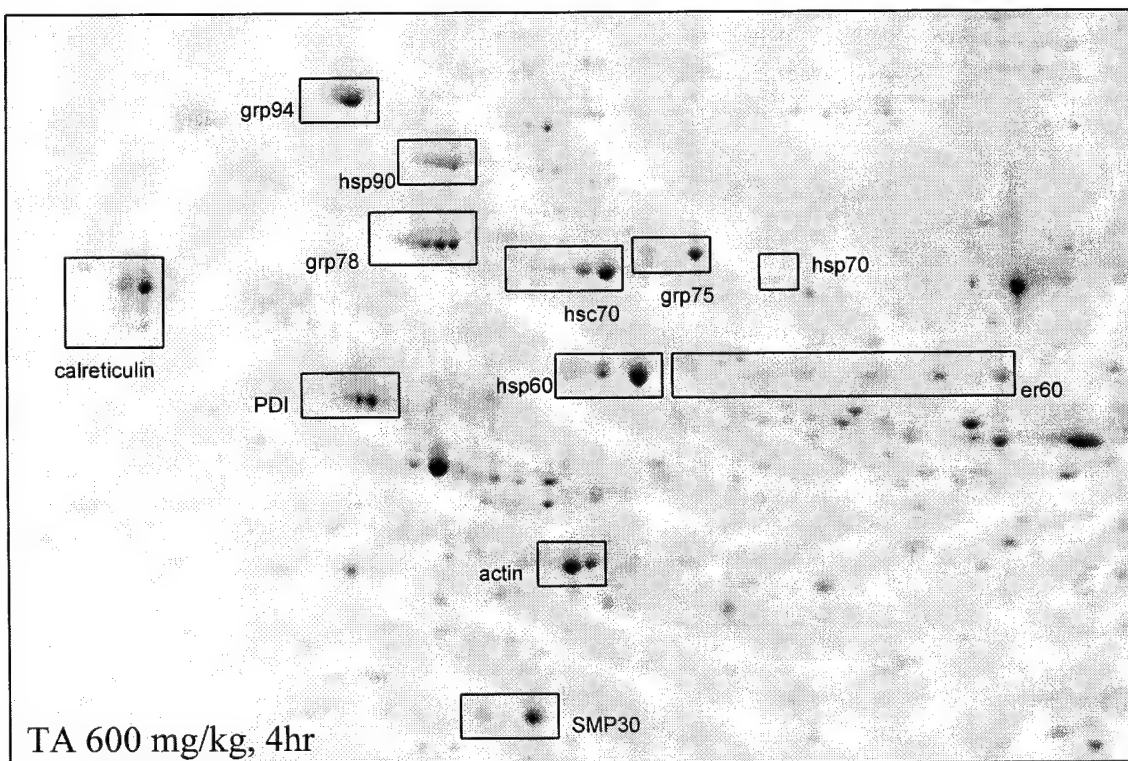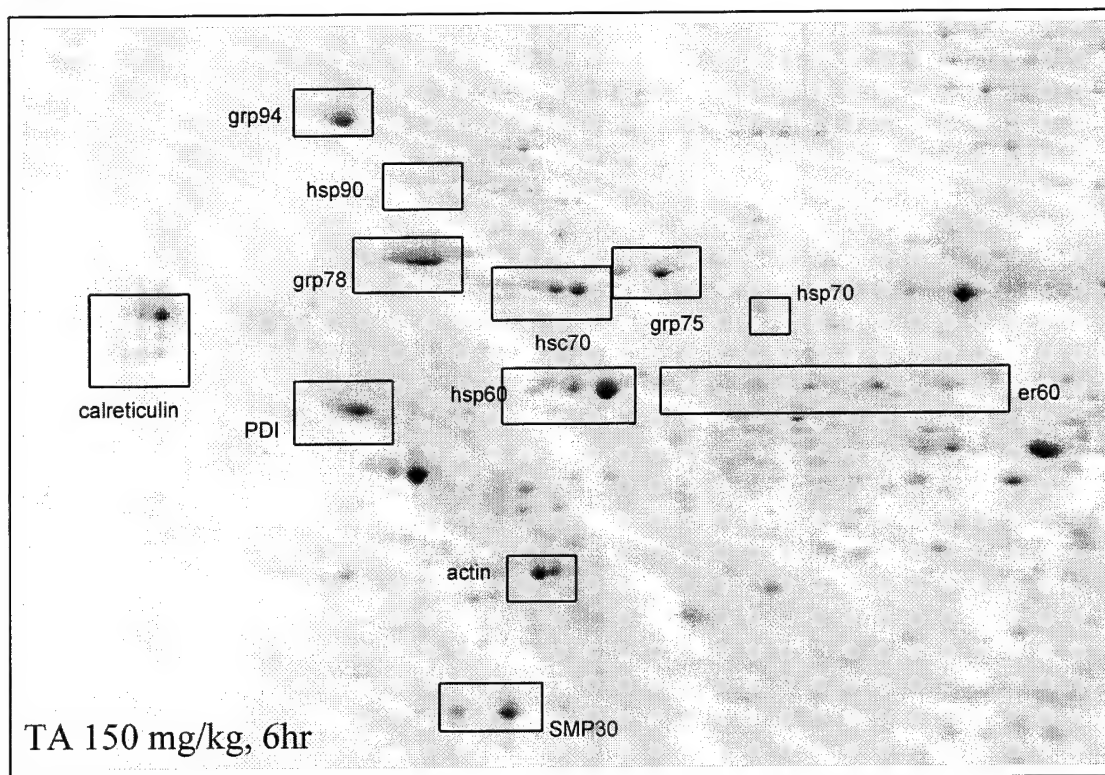
Figure 12. This figure illustrates a representative stained gel pattern (TIFF image) of a portion of the 2DE pattern of Sprague-Dawley liver homogenate containing the proteins studied. The pattern depicted in this figure was obtained from the liver of a rat treated with 600 mg/kg TA for 16 hr. Note the the increasing appearance of charge variants (leftward appearing spots) for calreticulin, grp78, ER60, hsc70 and PDI and the notable lack of effect on hsp60 and grp75.
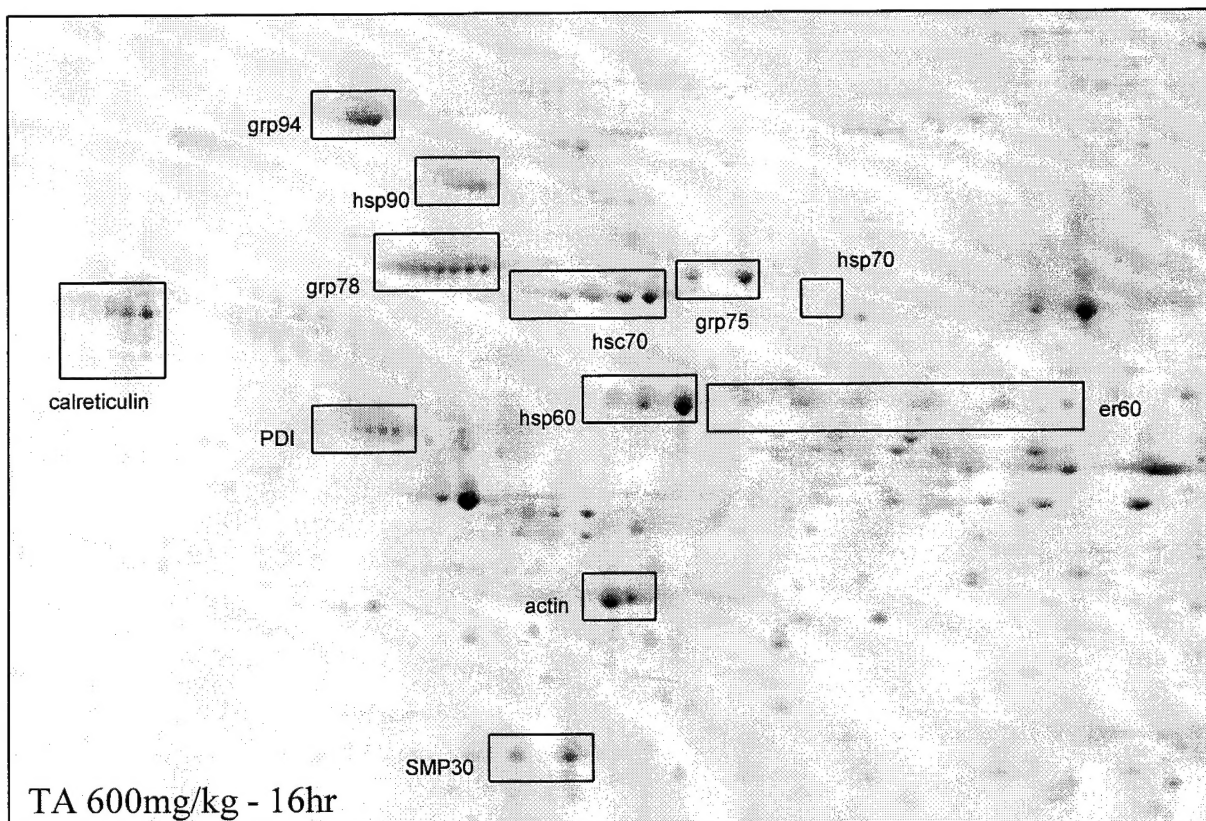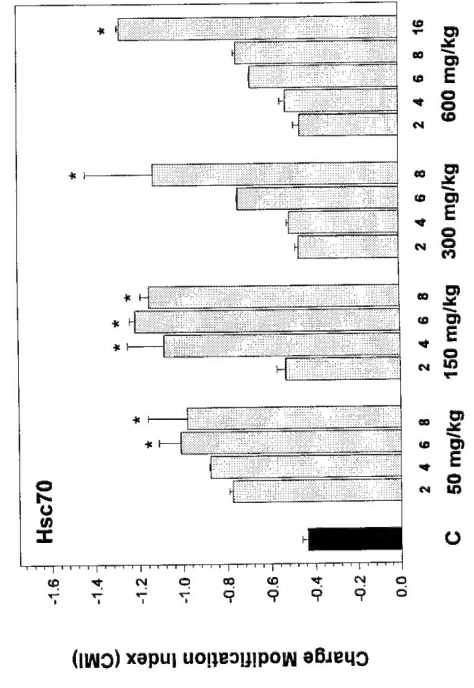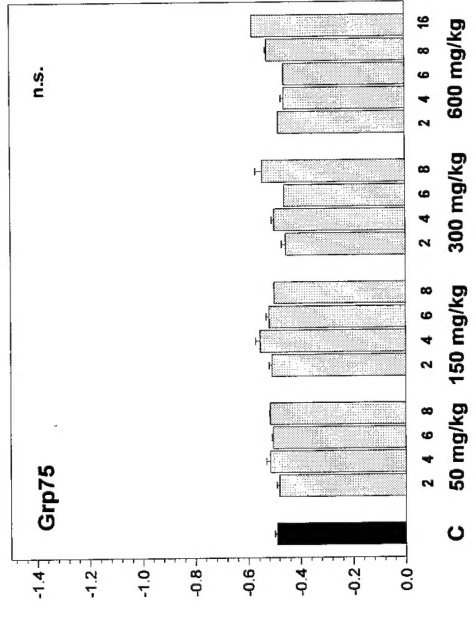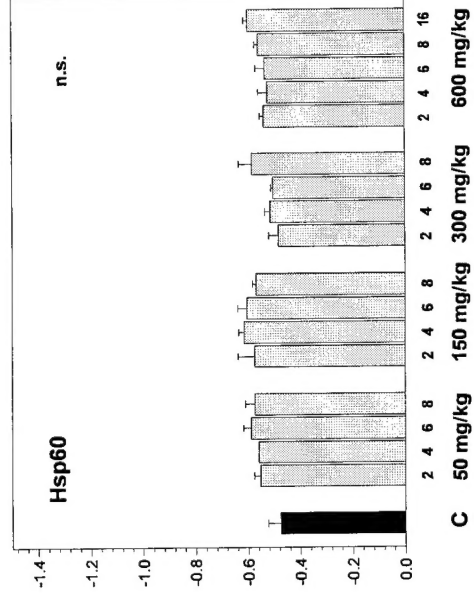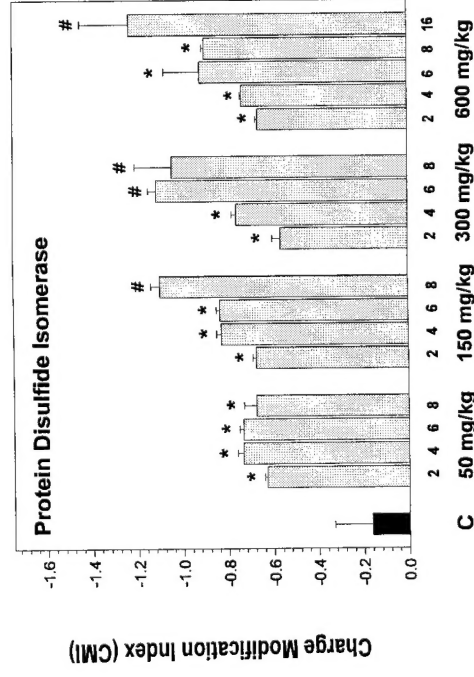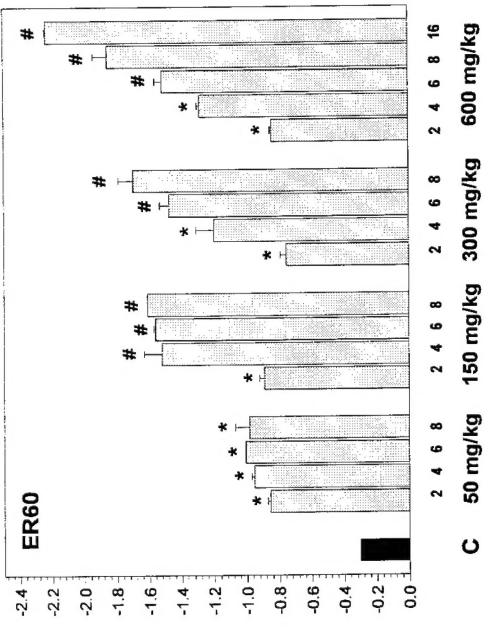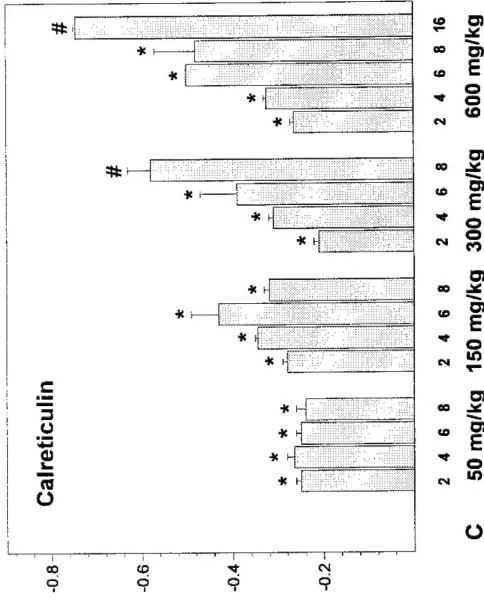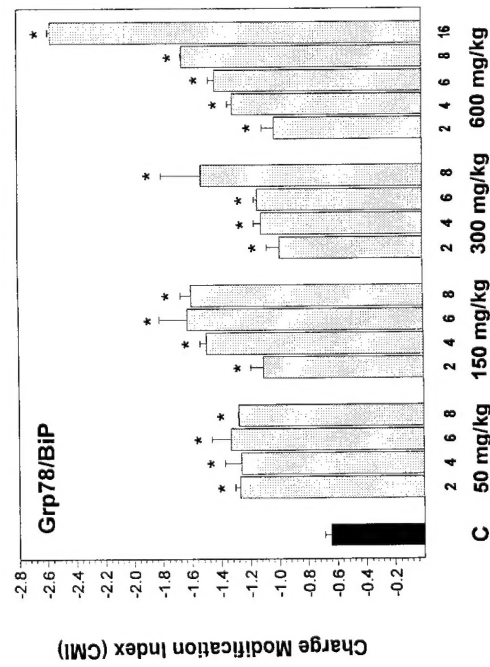
Figure 13. Charge Modification Indexes of the stress proteins/chaperones studied and their response to a twelve-fold dose range of TA administration for various durations. Bars represent means ± SE. # significantly different vs. vehicle-injected control, P<.05 via SNK multiple range analysis; # significantly different from 4 hr time point for each exposure, P<.05 via SNK multiple range analysis following ANOVA.

Appendix F

Publications:

Witzmann, F.A., B.M. Jarnot, D.N. Parker and J.W. Clack. (1994). Modification of hepatic immunoglobulin heavy chain binding protein (BiP/Grp78) following exposure to structurally diverse peroxisome proliferators. *Fundamental and Applied Toxicology* **23**, 1-8.

Witzmann, F.A., B.M. Jarnot and J.W. Clack. (1994). Charge modification in rodent hepatic Grp78/Bip following exposure to structurally diverse peroxisome proliferators. *Applied and Theoretical Electrophoresis* **4**, 81-88.

Witzmann, F.A., J.W. Clack, C.D. Fultz and B.M. Jarnot. (1995). Two-dimensional electrophoretic mapping of hepatic and renal stress proteins. *Electrophoresis* **16**, 451-459.

Witzmann, F.A., J. Lipscomb and C.D. Fultz. (1995). Comparative 2D-electrophoretic mapping of human and rodent hepatic stress proteins as potential biomarkers. *Applied and Theoretical Electrophoresis* **5**, 113-117.

Anderson, N.L., R. Esquer-Blasco, J.P. Hofmann, L. Meheus, J. Raymakers, S. Steiner, F. A. Witzmann and N.G. Anderson. (1995). An updated two-dimensional gel database of rat liver proteins useful in gene regulation and drug effects studies. *Electrophoresis* **16**, 1977-1981.

Witzmann, F.A., C.D. Fultz and J.C. Lipscomb. (1996). Toxicant-induced alterations in two-dimensional electrophoretic patterns of hepatic and renal stress proteins. *Electrophoresis* **17**, 198-202.

Witzmann, F., M. Coughtrie, C. Fultz and J. Lipscomb. (1996). Effect of structurally diverse peroxisome proliferators on rat hepatic sulfotransferase. *Chemico-Biological Interactions* **99**, 73-84.

Witzmann, F.A., C.D. Fultz, R.S. Mangipudy, and H.M. Mehendale. (1996). Two-dimensional electrophoretic analysis of compartment-specific hepatic protein charge-modification induced by thioacetamide exposure in rats. *Fundam. Appl. Toxicol.* **31**, 124-132.

Appendix G

Presentations:

Witzmann, F.A., J.W. Clack, B.M. Jarnot, and D.N. Parker. Modifications in BiP following exposure to structurally diverse peroxisome proliferators detected by two-dimensional electrophoresis. Presented at the Electrophoresis '93 Meeting, Wild Dunes Resort, Charleston SC, Nov 7-10, 1993

Application of 2D electrophoresis and image analysis to perfluorocarboxylic acid toxicology, Large Scale 2-D User's Conference and Workshop, September 8-10, 1993, Center for Advanced Biotechnology Research, Rockville MD

Presented a Seminar to faculty and students in the IUPUI Dept. Of Biology: "Two-dimensional Electrophoretic Applications in Toxicology," April 22, 1994

Witzmann, F.A., J.W. Clack and C.D. Fultz. Hepatic and renal stress proteins as biomarkers of chemical intoxication. *The Toxicologist* 15:50, 1995. Presented at the 34th Annual Meeting of the Society of Toxicology, Baltimore MD, March 5-9, 1995.

Witzmann, F.A., C.D. Fultz and J. Lipscomb. 2D-Electrophoretic mapping of human hepatic stress proteins as biomarkers of chemical intoxication. *Proceedings of the 1995 Tri-service/EPA/ATSDR Toxicology Conference*, 1995.

Witzmann, F.A., C.D. Fultz and J. Lipscomb. Comparative 2D-electrophoretic mapping of human and rodent hepatic stress proteins as potential biomarkers. *Proceedings of the Electrophoresis '95 Meeting*, Rockville MD, March 19-22, 1995.

Witzmann, F.A. Two-dimensional protein pattern recognition in chemical toxicity. *AFOSR Predictive Toxicology Program Review*, Fairborn OH, May 30-June 1, 1995.

Witzmann, F., C. Fultz and H. Mehendale. 2D-PAGE analysis of compartment-specific hepatic protein charge-modification induced by thioacetamide. *Proceedings of the International Electrophoresis '95 Meeting*, Pasteur Institute, Paris, France, August 29-Sep 2, 1995.

Mehendale, H.M., C.D. Fultz, R.S. Mangipudy, and F.A. Witzmann. 2D-Electrophoretic analysis of thioacetamide-induced protein charge modification in rat liver. The Toxicologist **30**, 83. Presented at the 35th Annual Meeting of the Society of Toxicology, Anaheim, CA, March 10-14, 1996.

Witzmann, F.A., C.D. Fultz and J.F. Wyman. 1,3,5-Trinitrobenzene toxicity in bovine testicular tissue-slices: two-dimensional electrophoretic analysis. The Toxicologist **30**, 119. Presented at the 35th Annual Meeting of the Society of Toxicology, Anaheim, CA, March 10-14, 1996.

Mangipudy, R.S., P.S. Rao, A. Warbritton, T.J. Bucci, F.A. Witzmann, and H.M. Mehendale. Dose-dependent modulation of cell death: apoptosis vs. necrosis in thioacetamide toxicity. The Toxicologist **30**, 164. Presented at the 35th Annual Meeting of the Society of Toxicology, Anaheim, CA, March 10-14, 1996.